INTERNATIONAL JOURNAL OF HYDROGEN ENERGY 41 (2016) 14387–14403

Available online at www.sciencedirect.com

ScienceDirect

journal homepage: www.elsevier.com/locate/he

Review Article

Recent progress in magnesium borohydride $Mg(BH_4)_2$: Fundamentals and applications for energy storage

*Olena Zavorotynska**, *Abdelouahab El-Kharbachi*, *Stefano Deledda*, *Bjørn C. Hauback*

Physics Department, Institute for Energy Technology, P.O. Box 40, NO-2027, Kjeller, Norway

ARTICLE INFO

Article history:
Received 10 December 2015
Received in revised form
2 February 2016
Accepted 2 February 2016
Available online 11 March 2016

Keywords:
Magnesium borohydride
Hydrogen storage
Batteries
Decomposition pathway
FTIR

ABSTRACT

Magnesium borohydride ($Mg(BH_4)_2$) shows interesting properties both from fundamental and applicative points of view. $Mg(BH_4)_2$ has the most complex crystal structures and the largest number of phase polymorphs among other borohydrides. Some of these polymorphs possess a significant porosity, and on the other hand ultra-density with the second highest volumetric hydrogen content among all known hydrides. Additionally, $Mg(BH_4)_2$ demonstrates the lowest theoretical stability, the lowest temperature of hydrogen release, and the mildest conditions for partial rehydrogenation among the alkali and alkaline-earth borohydrides. $Mg(BH_4)_2$ could also be of interest in batteries applications, since Mg metal holds better volumetric capacity and is more abundant than Li. In this work we review recent results on synthesis, structure, hydrogen storage properties and battery-related applications of $Mg(BH_4)_2$.

Contents

Introduction 14388
Synthesis and structure of $Mg(BH_4)_2$ 14389
Synthesis 14389
Solvent-based chemistry routes 14389
Solvent-free chemistry 14389
Polymorphism, phase transitions, and structural properties of $Mg(BH_4)_2$ 14390
Experimentally observed phases and phase transitions 14390
Theoretical structures 14391
Local structure of BH_4^- anions 14392

* *Corresponding author.*
E-mail addresses: olena.zavorotynska@ife.NO (O. Zavorotynska), Abdel.El-Kharbachi@ife.no (A. El-Kharbachi), stefano.deledda@ife.no (S. Deledda), bjorn.hauback@ife.no (B.C. Hauback).

http://dx.doi.org/10.1016/j.ijhydene.2016.02.015

Hydrogen desorption and absorption in $Mg(BH_4)_2$ 14394
Decomposition pathway 14394
Kinetics and thermodynamics of decomposition reactions 14396
Effect of additives on hydrogen storage properties of $Mg(BH_4)_2$ 14397
Other approaches for destabilization of $Mg(BH_4)_2$ 14397
$Mg(BH_4)_2$ for applications in batteries 14398
Summary 14398
Acknowledgments 14399
References 14399

Introduction

Present-day increasing energy demands, global environmental and political issues require at least partial substitution of fossil fuels with the energy coming from renewable sources. For transportation and on-demand usage wind or solar energy must be stored, and preferably in high-energy density media. A commercial whole hydrogen storage proton exchange membrane fuel cell (PEMFC) system and Li-batteries have comparable energy densities suitable for efficient electrochemical energy storage [1].

The extremely low density of H_2 gas at normal conditions is one of the main obstacles on the way for efficient energy storage in hydrogen media. The present commercial high energy-density solutions, such as liquid and pressurized hydrogen tanks, are associated with energy losses, expensive storage tanks, systems, and safety risks. Therefore alternatives, and in particular storage of chemically bonded hydrogen in metal hydrides, have been widely explored [2–8] and commercialized [1,9,10]. A hydrogen storage system must fulfill a wide range of requirements; the most important being high hydrogen content, fast kinetics of hydrogen desorption and absorption at low operating temperature (T) and pressure (p), and high purity of released hydrogen [11]. Metal borohydrides (MBHs) are complex hydrides containing hydrogen-rich molecular BH_4^- anions counterbalanced by metal cations. The gravimetric and volumetric hydrogen densities in these compounds are suitable even for the demanding on-board hydrogen storage applications (e.g, 18.5 wt% and 121 kg m^{-3} H_2 in $LiBH_4$ [12,13]). Alkali or alkaline-earth MBHs are stable ionic compounds, most of them decomposing above 300 °C with release of mainly H_2 [14].

Among the Group I and II MBHs, magnesium borohydride ($Mg(BH_4)_2$) displays very interesting properties both from fundamental and applicative points of view. It has the largest number of polymorphs with the complex structures comprising several hundred atoms in the unit cells. Some of these polymorphs possess unique for metal hydrides porosity and high specific surface area (SSA) [15,16], and others are ultra-dense with one of the highest volumetric hydrogen densities (147-145 g H_2/L at ambient conditions) among all known metal hydrides [15,17]. In addition, $Mg(BH_4)_2$ has one of the highest gravimetric hydrogen densities (14.5 wt% exceeded by only $LiBH_4$ and $Be(BH_4)_2$) and theoretically predicted hydrogen release at rather mild conditions [18,19]. It has also the lowest decomposition temperature (T_{dec}), and the mildest conditions for partial rehydrogenation demonstrated experimentally. In addition, $Mg(BH_4)_2$ could be of interest in batteries applications, since Mg metal holds better volumetric capacity (3833 mAh cm^{-3} compared to 2036 mAh cm^{-3} of Li) and is more abundant [20]. Despite of all these interesting properties, a review publication on $Mg(BH_4)_2$ has not appeared yet. The published results can be found in more than hundred articles. Thus this work reviews the recent (after 2006) findings on crystal structure, properties and applications of $Mg(BH_4)_2$.

The early studies on $Mg(BH_4)_2$ describe synthesis, structure and chemical properties of the compound, its adducts and solvates [21–28]. However, the interest in $Mg(BH_4)_2$ research renewed in early 2000's, when the compound was proposed for hydrogen storage [29–32]. During the last decade more than a hundred studies on $Mg(BH_4)_2$ have been published, compared to some twenty works for the preceding half a century. In 2011 a newly discovered cubic phase of $Mg(BH_4)_2$ was the first example of a high surface area complex hydride with a porous structure suitable for gas adsorption [15].

Here we focus mainly on experimental results although theoretical assessments are included when relevant. The review is organized as follows. Firstly we summarize briefly the synthetic approaches to obtain different polymorphs of $Mg(BH_4)_2$, the details are found elsewhere [30,33–35]. The structures and the vibrational properties of BH_4^- in these polymorphs are compared. The vibrational spectra characterize the local environment of the anions which is related to the stability of BH_4^- and consequently $Mg(BH_4)_2$. The infrared (IR) spectra of several polymorphs, obtained in our laboratory at identical conditions, are presented. The following part addresses the hydrogen storage properties of $Mg(BH_4)_2$. We summarize the studies on the decomposition pathway of $Mg(BH_4)_2$ and point out discrepancies that are found in the literature. The thermodynamics of H_2 release is also reviewed, and we present our data on the activation energy (E_a) of decomposition of the novel porous γ-$Mg(BH_4)_2$. The possibility of improving the H_2 release and absorption in $Mg(BH_4)_2$ with additives is considered. Finally the interest in magnesium borohydride for batteries applications is reviewed.

Synthesis and structure of $Mg(BH_4)_2$

Synthesis

Solvent-based chemistry routes

An interesting property of $Mg(BH_4)_2$ is its polymorphism which appears to be richer than that of any other Group I and II borohydrides. The hexagonal ($P6_122$) α [30,33–39], cubic (*Id*-3*a*) γ [15], orthorhombic β (*Fddd*) [35,37,40], trigonal ($P3_112$) ζ-$Mg(BH_4)_2$ [16] and amorphous $Mg(BH_4)_2$ can be all obtained with excellent yields by solvent-based syntheses, and both the α and γ phases are commercially available. In the synthesis of $Mg(BH_4)_2$, pure magnesium, magnesium halide, MgH_2, $Mg(C_4H_9)_2$, or $Mg(nBu)_2$ are used as the magnesium source, and B_2H_6, amine-boranes, alkyl-boranes, or $Al(BH_4)_3$ as the source of BH_4^- boron and hydrogen. The most common solvents for the synthesis are diethyl ether or hexane, although toluene and heptane were also successfully used [33]. Notably, the removal of the solvent at elevated temperatures, >100 °C, is a crucial step for obtaining crystalline material with the desired structure [30,34,37]. This step is even more critical when the solvent needs to be removed from the pores of γ-$Mg(BH_4)_2$ [41].

Solvent-free chemistry

Many attempts have been made in order to prepare $Mg(BH_4)_2$ via solvent-free synthesis methods which could be safer, more economic and environmentally friendly. Solvent-free synthesis of $Mg(BH_4)_2$ can be achieved through mechanical milling, hydrogenation at high *T* and H_2 pressure, gas–solid reaction between B_2H_6 and MgH_2, and a metathesis reaction between $MgCl_2$ and $LiBH_4$ [42,43]. Notably, a mechanochemical reaction of $2NaBH_4$+$MgCl_2$ allegedly lead to the formation of dual cation (Na,Mg)BH_4 [44].

Reactive mechanochemical synthesis from the elements with and without subsequent hydrogenation. The synthesis of $Mg(BH_4)_2$ from Mg + 2B and MgH_2 + 2B mixtures, milled for 50 h under 2 MPa of H_2, yielded magnesium hydride, boron and some Mg–B–H compounds with no experimental evidence for $Mg(BH_4)_2$ [45]. The mixtures released up to 3.9 wt% of H_2 in ~100 min when decomposed at 325 °C. MgB_2 milled under the same conditions did not contain any hydrogenated phases. After annealing for 120 h at 450 °C and 12 MPa of H_2, MgB_2 showed a minor (about 0.25 wt%) hydrogen absorption, and the Mg + 2B and MgH_2 + 2B pre-milled mixtures did not show any additional H_2 uptake. The same group have reported that the Mg + 2B mixture milled for 12 h in Ar and subsequently hydrogenated at up to 2.5 MPa H_2 and 300 °C resulted in the formation of MgH_2 only [46]. Partial hydrogenation of the pre-milled MgB_2 was, however, achieved by Severa et al. [47] who found 11 wt% uptake after hydrogen absorption at H_2 pressure of 90 MPa and 400 °C for 108 h. Li et al. reported 25% yield of $Mg(BH_4)_2$ after milling MgB_2 at 1 MPa H_2 for 10 h, followed by hydrogenation at 400 °C and 40 MPa H_2 for 24 h. Those results suggest that the hydrogenation of MgB_2 is a pressure-dependent reaction, and very high pressures are required to form $Mg(BH_4)_2$. Amorphous $Mg(BH_4)_2$ was synthesized from MgB_2 with a 50% yield by reactive milling under 10 MPa of H_2 for 100 h [48] and under 35 MPa H_2 for 50 h [49]. The latter synthesis yielded 4 wt% H_2 release after decomposing the hydrogenated sample below 390 °C. Kaya et al. reported that the synthesis of $Mg(BH_4)_2$ by milling Mg and B mixture in H_2 is feasible and pressure-dependent [50].

Direct rehydrogenation of decomposed $Mg(BH_4)_2$ and/or its decomposition reaction products. Rehydrogenation of the decomposition reaction products is crucial for the use of

Table 1 – Experimentally observed polymorphs of $Mg(BH_4)_2$ and their specific (ρ) and volumetric hydrogen (ρ_v) densities.

Phase	Space group	Z	Cell parameters, Å	Cell volume, Å^3	ρ, g cm^{-3}	ρ_v, g_{H2} L	Ref.
α-$Mg(BH_4)_2$	$P6_122$	30	a = 10.33555 b = 10.33555 c = 37.08910 α = β = 90° γ = 120	3431.21	0.783	117	[38]
β-$Mg(BH_4)_2$	*Fddd*	64	a = 37.04892 b = 18.49186 c = 10.85945 α = 90°	7439.82	0.76	113	[37]
γ-$Mg(BH_4)_2$	*Id*-3*a*	24	a = 15.7575 α = 90°	3912.57	0.55	82	[15]
	Ia-3*d*	24	a = 15.8234 α = 90°	3961.86	0.5431		[54]
δ-$Mg(BH_4)_2$[a]	$P6_3$		a = 8.35 c = 4.68	283.47			[55]
δ-$Mg(BH_4)_2$	$P4_2nm$	2	a = 5.4361 b = 5.4361 c = 6.1468 α = 90°	181.65	0.987	147	[15]
ζ-$Mg(BH_4)_2$[b]	$P3_112$	9	a = 10.424 c = 10.729 α = 90°	1009.7			[16]

[a] Indexed, no structural refinement.
[b] Isostructural to α-$Mn(BH_4)_2$ [56].

$Mg(BH_4)_2$ in hydrogen storage applications. The rehydrogenation of completely decomposed $Mg(BH_4)_2$ (to MgB_2) was reported to yield a mixture of β-$Mg(BH_4)_2$ and $MgB_{12}H_{12}$ [39]. The absorption reaction was carried out at 90 MPa of H_2 and 390 °C for 72 h. Forty three percent yield of β-$Mg(BH_4)_2$ after deuteration of MgB_2 and $Mg^{11}B_2$ at 80 MPa D_2 and 400 °C was achieved by Pitt et al. [51]. Li et al. reported 6.1 wt% H_2 uptake after rehydrogenation of decomposed $Mg(BH_4)_2$ [52]. The rehydriding reaction was conducted with a Sieverts apparatus at 270 °C in hydrogen at 40 MPa for 48 h. In addition to $Mg(BH_4)_2$, $MgB_{12}H_{12}$ was found among the reaction products. Thus, direct synthesis of $Mg(BH_4)_2$ from the elements under H_2 pressure has been shown feasible. However, further research is required in order to decrease reaction times and operating temperatures and pressures.

Gas-solid reaction with B_2H_6. Zhang et al. [53] reported the synthesis of Mg–B–H compounds from the reaction between MgH_2 and B_2H_6, the latter obtained by thermal decomposition of a $NaBH_4/ZnCl_2$ pre-milled mixture. The product, constituted by a mixture of crystalline MgH_2, Mg and some amorphous Mg–B–H, released only a negligible amount of H_2 before decomposition of MgH_2.

In conclusion, excellent yields of $Mg(BH_4)_2$ in various crystalline polymorphs can be obtained via solvent-based synthetic methods. The solvent-free routes typically yield lower amounts of $Mg(BH_4)_2$ with mixtures of other Mg–B–H byproducts or an alkali-metal halide forming from the BH_4^- source. The hydrogenation reactions from the elements require long time, very high H_2 p and T, although they can provide satisfactory yields. Reactions with utilization of B_2H_6 are rather impractical in view of toxicity and flammability of diborane. Nonetheless, the solvent-free synthesis has proven to be feasible and possibly can be improved.

Polymorphism, phase transitions, and structural properties of $Mg(BH_4)_2$

Experimentally observed phases and phase transitions

$Mg(BH_4)_2$ is characterized by a vast variety of experimentally observed and theoretically predicted crystal structures that are larger in number than for any other known borohydride. The experimentally observed phases of $Mg(BH_4)_2$ are summarized in Table 1 alongside with the densities relevant for hydrogen storage applications.

Some of the phases can be synthetized by solvent-based methods as described in the Section Synthesis, whereas others have been observed upon phase-transitions (see Table 2). For instance, α-$Mg(BH_4)_2$ transforms to the orthorhombic β-phase (*Fddd*) upon heating [30,32,37,38]. Therefore, those phases are also referred to as the low-temperature (LT) and high-temperature (HT) phase, respectively. The porous γ-$Mg(BH_4)_2$ undergoes thermally-induced phase transitions to ε [54,57,58] and, subsequently, to β′-$Mg(BH_4)_2$ (allegedly a disordered phase of β [54,57]). The ε-to-α phase transition upon cooling of ε-$Mg(BH_4)_2$ has been also reported [57,59], however, this is not always observed. For example, Fig. 1c shows the powder X-ray diffraction (PXD) pattern of (ε+β′)-$Mg(BH_4)_2$ mixture measured several hours after being cooled down to room temperature (RT). The structures for the ε- and

Table 2 – Experimentally observed polymorphic transitions in $Mg(BH_4)_2$.

Final phase	Reaction	Reaction atmosphere/comments	Ref.
ε, β′	$\gamma/(\gamma+am^*)/(\alpha^*+\gamma)/(am+\gamma^*)\text{-}Mg(BH_4)_2 \xrightarrow{125-225\,^\circ C} \varepsilon\text{-}Mg(BH_4)_2 \xrightarrow{155-275\,^\circ C} \beta'\text{-}Mg(BH_4)_2$	0.1 MPa Ar/0.1 MPa H_2/0.2 MPa He flow/0.25 MPa H_2/irreversible	[54,57,58,63]
β	$\alpha\text{-}Mg(BH_4)_2 \xrightarrow{>180\,^\circ C} \beta\text{-}Mg(BH_4)_2$		[30,32,37,38]
ζ	$Mg(BH_4)_2\ 1/2(CH_3)_2S \rightarrow \alpha\text{-}Mg(BH_4)_2 \xrightarrow{224\,^\circ C} \zeta\text{-}Mg(BH_4)_2$	0.1 MPa Ar	[16]
δ	$\alpha\text{-}Mg(BH_4)_2 \xrightarrow[RT]{1.5-3.35\ GPa,} \delta\text{-}Mg(BH_4)_2$	Di anvil cell, irreversible upon decompression at RT	[55]
δ	$\alpha\text{-}Mg(BH_4)_2 \xrightarrow[RT]{1.1-1.6\ GPa,} \delta\text{-}Mg(BH_4)_2$	Di anvil cell, reversible at 0.1 MPa, 100 °C	[15]
	$\alpha\text{-}Mg(BH_4)_2 \xrightarrow[RT]{0.4-0.9\ GPa,} \delta\text{-}Mg(BH_4)_2$	Di anvil cell	[15]
	$\gamma\text{-}Mg(BH_4)_2 \xrightarrow[RT]{2.1\ GPa,} am\text{-}Mg(BH_4)_2 \xrightarrow[RT]{} \delta\text{-}Mg(BH_4)_2$		

*-minor amount; am – amorphous.

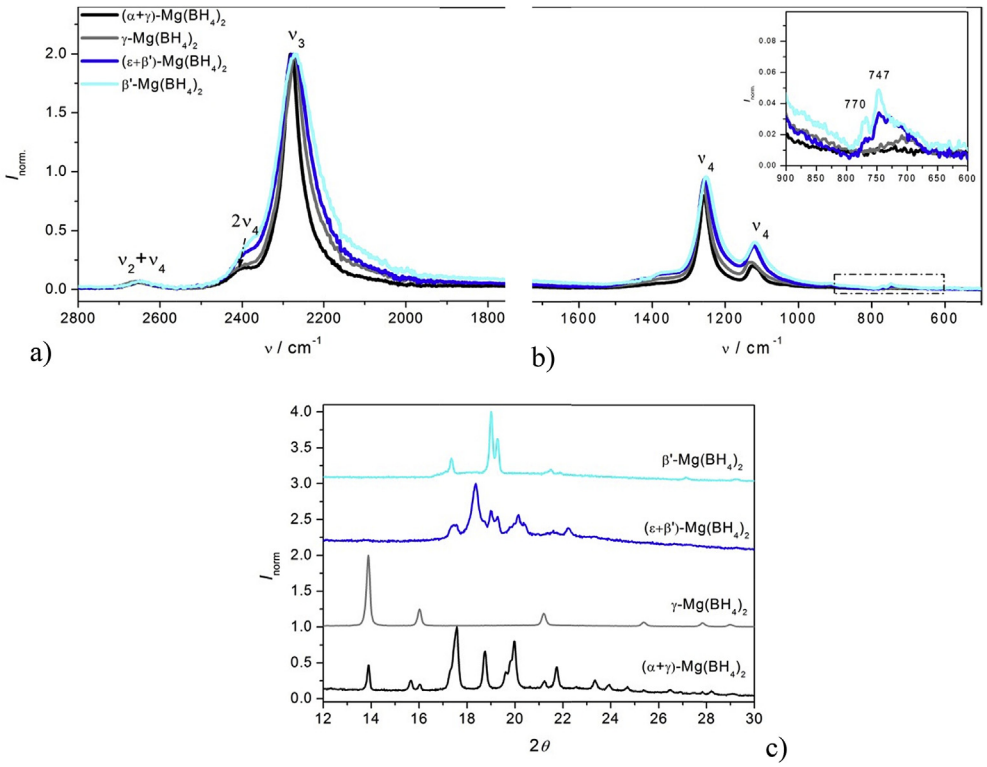

Fig. 1 – (this work). IR spectra of α-, ε+β′-, β′-, and γ-$Mg(BH_4)_2$: a) B–H stretching region; b) B–H bending region. The inset on Fig. 1b is discussed in the Section Decomposition pathway. c) PXD patterns of the samples. IR spectra were collected in the ATR mode upon a diamond crystal with 2 cm^{-1} resolution. PXD data were obtained in a Debye-Scherrer geometry using Cu Kα radiation (λ = 1.5418 Å) and rotating glass capillaries at RT. The PXD and IR data were obtained within 2 h after preparation of β′ and ε+β′ phases. The ε+β′-, β′-$Mg(BH_4)_2$ were obtained by heating γ-$Mg(BH_4)_2$ in 50 ml min^{-1} Ar flow till 175 and 212 °C, respectively, at 5 K/min without isothermal step.

β′-phases have not been published, and the phases were identified by comparison to the literature [58], [54,57]. The phase-transitions to the HT-$Mg(BH_4)_2$ phases are irreversible. Indeed, β-$Mg(BH_4)_2$ or β′ have also been found after rehydrogenation of $Mg(BH_4)_2$ [39,47,60–62]. The high-density δ-$Mg(BH_4)_2$ polymorph can be obtained upon compression of the α and γ-phases [15,55]. This high pressure phase is much simpler than the α and γ-polymorphs (Table 1). It is preserved after pressure release but upon heating to 100 °C, it transforms to α either γ starting phase [15]. Some intermediate phases were also observed upon compression of the α-, and γ-polymorphs [15]. Besides the crystalline phases, amorphous $Mg(BH_4)_2$ can be obtained via solvent-free synthesis methods (see Section Solvent-free chemistry), mechanical milling of crystalline phases [15,31,63], and pressure collapse of the porous γ-$Mg(BH_4)_2$ [17].

Porous frameworks. γ-$Mg(BH_4)_2$ is an intriguing first example of porous high surface area complex hydride, although α-$Mg(BH_4)_2$ also possesses some open voids large enough to accommodate small molecules such as H_2O [15]. The reported values of the specific surface area (SSA) for γ-$Mg(BH_4)_2$ vary greatly, being 60 [64] and 1160 m^2 g^{-1} [15], respectively. However, the authors of ref. [64] noted that the non-equilibrium measurements conditions used in their work could have been responsible for the low obtained value of SSA. Despite these discrepancies, it was shown that the open porous structure of γ-$Mg(BH_4)_2$ can adsorb small molecules [15,64,65] and significantly enhances the D-H isotopic exchange rates [66]. Due to the elevated rates of D-H isotopic exchange, the metastable intermediate ε-$Mg(BH_4)_2$ was also suggested to possess an intrinsic porosity [66]. Finally, the recently described ζ-$Mg(BH_4)_2$, too, was reported to have an open porous structure [16]. This unique combination of hydride properties and high surface area opens up new possible applications where surface effects are important.

Theoretical structures

Numerous theoretically predicted structures of $Mg(BH_4)_2$ have been published [18,19,29,67–75], showing an "outstanding discrepancy between experiment and theory" [72]. For example, first-principle studies found that the high-pressure structures *P*-4, *I*4$_1$/*acd* [73], *I*4$_1$/*amd* [74], *Fddd* [75] are more favorable than the experimentally determined *P*4$_2$*nm* phase of the ultra-dense δ-$Mg(BH_4)_2$ [15]. Similarly, several alternative structures have been proposed for the ground-state LT-$Mg(BH_4)_2$ [18,19,29,67,69–71] with only few results agreeing with the experimental *P*6$_1$22. An important consequence of these discrepancies can be an erroneous assessment of the thermodynamic parameters which can affect the evaluation of the hydrogen storage properties of $Mg(BH_4)_2$. It was suggested [72,76] that the small size of the Mg cation and the

consequent close proximity of BH_4^- lead to increased repulsive interactions and to a situation where the orientation of the anions plays an important role. This results in a variety of equivalent crystalline symmetries that are degenerate in energy, similarly to oxides such as silica [76]. The authors in Ref. [76] noted the possibility of formation of 3D networks with large cavities before the porous γ-$Mg(BH_4)_2$ was discovered and in fact some of the predicted structures are also highly porous, as noted in Ref. [15]. The authors of ref. [15] have also argued that the essential reason for rich polymorphism in $Mg(BH_4)_2$ is a partial covalent bonding between Mg^{2+} and BH_4^-. Bil et al. [72] have demonstrated that the long-range dispersive interactions in γ-$Mg(BH_4)_2$ are non-negligible. Taking into account these effects, they showed that the experimental α-$Mg(BH_4)_2$ with space group $P6_122$ is favored over a large set of polymorphs. However, among their 36 calculated structures, no porous γ-$Mg(BH_4)_2$ (not known yet at the time of their publication) was reported, although the β-$Mg(BH_4)_2$ was predicted. More accurate DFT calculations have helped in the correct identification of α-$Mg(BH_4)_2$ structure [67], which was first reported as $P6_1$ [36,37] and later revised into $P6_122$ [38] in agreement with the DFT study [67]. It can be concluded then that because of the complex structures of the $Mg(BH_4)_2$ polymorphs, accurate theoretical calculations are challenging and require high precision of the simulation method accounting for the dispersive interactions and including the long-range effects. At the same time, also dynamic effects may be responsible for the significant discrepancy between theoretical and experimental structures.

Local structure of BH_4^- anions

The local structure of BH_4 can be related to the stability of the compounds and can be characterized with vibrational spectroscopy studies. Free molecular BH_4 ions have high tetrahedral (T_d) symmetry and four normal modes of vibrations: symmetric stretching and bending, ν_1 (A_1, Raman-active (R)) and ν_2 (E, R); asymmetric stretching and bending, ν_3 (F_2, IR-active (IR), R) and ν_4 (F_2, IR, R), respectively. The *E* mode is doubly degenerate, while the *F* mode is triply degenerate. In solids the inactive modes can activate and the degenerate modes can split due to various solid-state effects. IR and Raman spectra of various borohydrides have proven to be characteristic of the compound since they are sensitive to the site symmetry, crystal field and cation effects, Fermi resonances, and the ^{10}B isotopic effect [77–82].

As described above most of $Mg(BH_4)_2$ polymorphs have complex structures with hundreds of atoms in the unit cell and boron on several nonequivalent symmetry sites. The site symmetries of BH_4 are low, which is expected to cause the splitting of all the degenerate modes, and thus giving rise to nine modes of vibrations per BH_4 [83]. Calculated Raman spectra of the $P6_122$ phase [67] reflect this complexity. Taking into account also the Fermi resonances and isotopic effects, one would expect several tens of peaks in the IR and Raman spectra of $Mg(BH_4)_2$. However, the experimental RT IR spectra of various polymorphs of $Mg(BH_4)_2$ are remarkably simple and similar to each other (Fig. 1 and Table 4). Fig. 1 shows as an example the IR spectra of as synthesized α- and γ-$Mg(BH_4)_2$ and the ε+β′-, β′-, modifications obtained from γ-$Mg(BH_4)_2$. The spectrum of α-phase is characterized mainly by stretching at 2277 ± 4 cm^{-1} (ν_3), and bending at 1258 ± 2 and 1117 ± 9 cm^{-1} (ν_4) (Table 4). The latter weaker peak is broader and seems to be composed by at least two components (at 1124 and 1110 cm^{-1}). Splitting in the ν_3 mode and more peaks in the bending region have been reported [30,38], which might be due to the measurement method in KBr pellets and impurities, respectively. These data are not taken into account when calculating the mean values for the peak positions presented in Table 4. The IR spectra of γ- and ε-$Mg(BH_4)_2$ are very similar to those of the α-phase (Fig. 1 and Table 4) whereas those of β′ are slightly red-shifted. More differences in peak shapes and positions can be drawn from the Raman spectra (see Table 4 for references) and the low-temperature measurements. The measurements of single crystal α-$Mg(BH_2)_2$ [84] and polycrystalline α- and β-phases at cryogenic *T* [85] demonstrated considerable splitting of the peaks and differences between the vibrations of the two phases.

Raman spectra of crystalline polymorphs show more intense and narrow peaks with respect to the amorphous phase [17,38,63]. The B–H stretching and bending regions are very similar in all polymorphs, as well as the geometries and local environment of BH_4 (Table 3). This can also suggest the comparable stability of the B–H bonds in the polymorphs.

Raman spectroscopy in combination with PXD was applied in order to study the pressure-induced transformations in LT-, HT-$Mg(BH_4)_2$ and the high pressure polymorph [55]. It was shown that upon compression both LT- and HT-$Mg(BH_4)_2$ undergo similar transformations with significant shift and splitting of the peaks in the spectra. These modifications were assigned to the phase transitions. The Raman spectra of the high-pressure phase appeared to be more complex than of the low-pressure phases, indicating a distortion in the local geometry of the BH_4 ions.

The lattice modes have been studied by inelastic neutron scattering (INS) [85,86], Raman and Far IR (FIR) spectroscopies. The FIR and Raman data are summarized in Table 4. The reorientational motions of BH_4 in the α, β, γ-, and amorphous (pressure-collapsed γ-) polymorphs were studied by ^1H and ^{11}B-MAS-

Table 3 – BH_4^- molecular geometry and local environment in $Mg(BH_4)_2$.

Phase	Space group	*d* (B–H), Å	(HBH) angles, °	d_{min} (H···H), Å	Orientation BH_4^-···Mg, d (H···Mg), Å	Ref.
α	$P6_122$	1.15–1.30	104.2–112.9	1.88	Bidentate, 1.92–2.16	[38]
β	*Fddd*	1.23	109.5	1.99	Bidentate, 1.90–2.19	[37]
γ	*Id-3a*	1.22	109.4–109.5	1.99	Bidentate, 1.96, 2.00	[15]
	Ia-3d	1.22	109.4–109.5		Bidentate, 1.95, 2.05	[54]
δ	$P4_2nm$	1.21	109.1–110.2	1.73	Bidentate, 1.96, 2.01, 2.14	[15]
		1.22				

Table 4 – Experimentally observed infrared (IR) and Raman (R) peaks of $Mg(BH_4)_2$ (at RT). If not mentioned, the tentative assignment of the peaks was performed within this work.

Phase		Observed peaks and assignment						Ref.
		ν_1	ν_2	ν_3	ν_4	Combin./Overt.	Lattice	
α	R	n/i	1392	n/i	1208–1195*	n/i	525,445, 266,199,169†	[15]
	IR			2275	1257, 1124–1111	n/i		[15]
	R		1395		1199	2199		[38]
	IR		1391	2274	1258 1104-1018†† –1032		795††	[38]
	R	2332 &&	1390	2297	1208, 1191 1122	2400, 2194	600-430, 344, 256, 207, 200, 170	[85]†, &
	IR			2384 2292 2223	1261, 1126			[30]
	R	2308	1388, 1310w, 1288w	2283	1205, 1190, 1126, 1088, 1039	2334	670, 248, 204, 195, 172†	[36]
	R	2301	1392		1208-1195	2195		[86]
	IR			2275	1258, 1124-1112			[86]
	R	2304	1390		1200	2500, 2202		[87]
	IR			2282	1258, 1127-1110sh	2650, 2400		this work**
mean α	R	2304 ± 4	1391 ± 2					
	IR			2277 ± 4	1258 ± 2, 1117 ± 9			
β	R	2300	1390		1210			[31]
	IR			2269	1252,1119			[38]
	IR		1400 (?)	2384 2292 2223 ¥	1262, 1125			[30]
β′	IR		~1370br (?)	2267	1250, 1120	2645, ~2385		This work
ε**	IR		~1370br (?)	2274	1256, 1120	2649, 2394		This work
γ	R	2321	1404	2270	1192	2535 2209		[66]
	IR		~1370br (?)	2270	1260,1128-1100sh	2660, ~2400		[66]
	IR		~1370br (?)	2271	1260,1128	2660		This work
	IR			2267	1259		434, 409, 257, 231 (FIR)	[59]
	R	2317	1403		1191	2530 2206		[17]
mean γ	R	2319 ± 3	1403.5 ± 0.7					
	IR			2270 ± 2	1120 ± 10			

n/i – not indicated; * peaks appearing as doublets are marked with "-"; † assignment by the authors, †† possibly impurities; sh – shoulder; br – broad, w – weak; ** contains small amount of γ-phase, & contains small amount of β-phase; && not accounted for in the mean value; ¥ measured as KBr pellet; FIR – Far IR.

NMR [17,88–91]. It was shown that the parameters of reorientational motion in all phases strongly differ from each other, and each of the phases is characterized by distinct distribution of activation energies for the BH_4 reorientations. For the α-phase, three values of the activation energy were measured corresponding to three coexisting reorientational processes [89]. In other phases only one type of reorientational motion has been detected [17,90]. The fastest reorientational motion was observed for β-$Mg(BH_4)_2$ which was related to slightly longer H···H distances in the MgH_8 polyhedra of the β-phase [90].

Hydrogen desorption and absorption in $Mg(BH_4)_2$

The renewed interest in $Mg(BH_4)_2$ was fueled primarily by its potentially attractive hydrogen storage properties. The theoretical gravimetric hydrogen capacity, 14.9 wt%, is slightly lower than for $LiBH_4$ (18.5 wt%) [12], but still higher than the targets for on-board hydrogen storage [92]. The relation between the heats of formation and cation electronegativity for the borohydride compounds have indicated that $Mg(BH_4)_2$ should have the decomposition temperature between those of Group I (stable) and transition-metal (unstable at RT) borohydrides [29]. The follow-up experimental work have shown that pure crystalline $Mg(BH_4)_2$ had indeed interesting properties releasing mostly pure H_2 below 300 °C [30–32,52,93,94]. This is the lowest T_{dec} amongst the stable borohydrides. The subsequent DFT studies proposed that H_2 desorption from α-$Mg(BH_4)_2$ [19] and the hypothetical *I*-4*m*2 phase [18] should be feasible within 20–75 °C via the reaction $Mg(BH_4)_2 \rightarrow MgB_2 + 4H_2$ with $\Delta H = -38$–54 kJ mol^{-1} H_2^{-1}, and thus giving hope for an ideal hydrogen storage material. However, the preceding and subsequent experimental studies [95–98] had been persistently demonstrating decomposition above 200 °C via at least a two-step pathway. Those results prompted reconsidering the theoretical findings in view of the kinetic barriers and/or intermediate decomposition phases unaccounted for in the calculations [99], and encouraged search for the alternative decomposition reaction pathways both in theory and experiment.

The actual hydrogen storage properties of $Mg(BH_4)_2$ are defined by the experimental reaction pathway, the details of which are still debated. The following section summarizes the status on the decomposition reaction of $Mg(BH_4)_2$. We will also describe the progress in the reversibility of the hydrogen release reaction and the effect of additives on the decomposition and rehydrogenation of $Mg(BH_4)_2$.

Decomposition pathway

The decomposition reaction pathways of α and β [30–32,52,93,95–98], γ [54,57–59], ζ-$Mg(BH_4)_2$ [16], am-$Mg(BH_4)_2$ (amorphous) [29,42,43,63] and their mixtures have been studied extensively by different experimental approaches. However there are still some discrepancies in the results. The experimental findings have agreed that α-$Mg(BH_4)_2$ transforms to β-$Mg(BH_4)_2$, whereas γ, ζ, and am-$Mg(BH_4)_2$ (disordered γ-$Mg(BH_4)_2$) phases undergo the irreversible phase transitions through ε to β′-$Mg(BH_4)_2$ prior to decomposition [54,57,58] (see also Table 2). The mixture (α+γ)-$Mg(BH_4)_2$ was observed to form yet another unidentified phase before conversion to β′ [59]. Fig. 2 shows our new DSC-TGA measurements of the thermal decomposition of highly crystalline γ-$Mg(BH_4)_2$. PXD pattern of this sample is shown in Fig. 1. The endothermic events 1–2 in the 145–210 °C region are due to the γ→ε→β′ phase transitions in accordance to the described earlier findings. Decomposition of $Mg(BH_4)_2$ thus begins from the β- or β′-phases.

The first disagreement is related to the T_{dec} of $Mg(BH_4)_2$. It has been repeatedly shown that the onset T_{dec} is above 200 °C if the initial phase (at RT) is α-$Mg(BH_4)_2$, β-$Mg(BH_4)_2$ [30–32,52,93,95–98], or amorphous $Mg(BH_4)_2$ synthetized by ball-milling and hydrogenation of the $2LiBH_4 + MgCl_2$ mixture [43]. However, a small weight loss below 200 °C was reported for the am-$Mg(BH_4)_2$ [29], and for α-$Mg(BH_4)_2$ in the α→β phase transition *T* range [94]. For the porous γ-$Mg(BH_4)_2$ the weight loss has been observed at significantly lower temperatures, i.e. close to 100 °C [54,58,62]. In the data obtained in this work, a significant desorption starts at <150 °C, see Fig. 2a. Chong et al. [100] reported 2.5 wt % desorption for the sample decomposed at ~200 °C with very slow kinetics. However, recently Vitillo et al. argued that H_2 release from γ-$Mg(BH_4)_2$ does not begin until 200 °C, and that the weight loss observed below these temperatures should be associated with desorption of

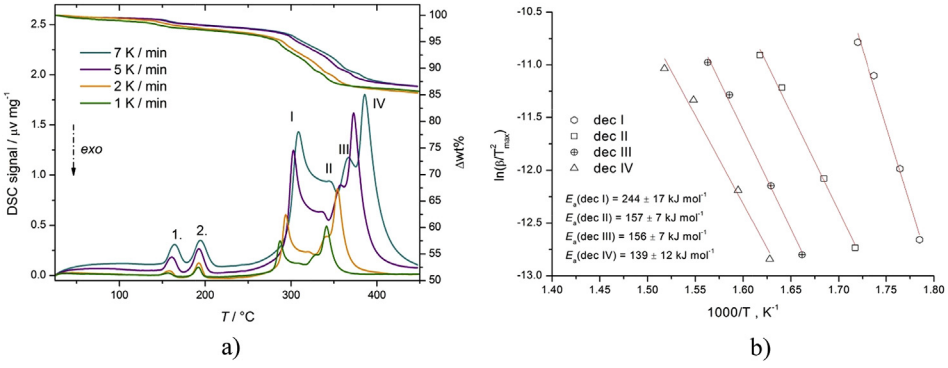

Fig. 2 – (this work): a) DSC-TGA measurements of γ-$Mg(BH_4)_2$ at various heating rates; steps 1–2 indicate phase transitions, and I–IV – decomposition; b) determination of the E_a of the I–IV decomposition steps with Kissinger method. Errors are obtained as the SD of the linear fits. The DSC-TGA measurements were performed with instrument Netzsch STA 449 F3 Jupiter in a 50 mL/min Ar flow.

Table 5 – Experimentally observed reaction products and/or decomposition pathways suggested for $Mg(BH_4)_2$.

No.	Decomposition reaction(s)	Comments	Ref.
1.	am[a]-$Mg(BH_4)_2 \rightarrow MgH_2 + 2B + 3H_2$	TPD	[29]
2.	α-$Mg(BH_4)_2 \rightarrow MgH_2 + 2B + 3H_2 \rightarrow Mg + 2B + 4H_2 \rightarrow MgB_2 + 4H_2$	In-situ PXD in vacuum	[30]
3.	$4Mg(BH_4)_2 \rightarrow Mg + 2MgB_4 + MgH_2 + 15H_2$	Rapid heating in vacuum till 390 °C + 30 min at 390 °C, ex-situ PXD	[30]
4.	β-$Mg(BH_4)_2 \rightarrow$ intermediate steps $\rightarrow MgH_2 + 2B + 3H_2 \rightarrow Mg + 2B + 4H_2 \rightarrow MgB_2 + 4H_2$	DSC-TGA, ex-situ PXD, He flow	[31]
5.	α-$Mg(BH_4)_2 \xrightarrow{>245\ ^\circ C} MgH_2 + Mg \xrightarrow{ca.\ 440\ ^\circ C} Mg$	In-situ PXD in dynamic vacuum	[32]
6.	α-$Mg(BH_4)_2 \xrightarrow{step\ I-II,\ 305\ ^\circ C} Mg$ + amorphous phases (melt ?) $\xrightarrow{step\ III,\ 335\ ^\circ C} MgH_2 + Mg$ + amorphous phases $\xrightarrow{step\ IV,\ 410\ ^\circ C} Mg$ + amorphous phases $\xrightarrow{step\ V,\ 580\ ^\circ C} MgB_2$	5 steps, HP-DSC, TG-DTA-MS, ex situ PXD, in He flow, 0.5 MPa He; 0.5, 1, 5 MPa H_2	[94]
7.	$Mg(BH_4)_2 \xrightarrow{>450\ ^\circ C,\ vacuum} MgB_{12}H_{12}$	^{11}B-SS-NMR ^{11}B-D_2O-NMR ^{1}H- D_2O-NMR	[108]
8.	β-$Mg(BH_4)_2 \rightarrow 1/6\ MgB_{12}H_{12} + 5/6\ MgH_2 + 13/6H_2 \leftrightarrow MgH_2 + 2B + 3H_2 \leftrightarrow Mg + 2B + 4H_2$	Raman, TG, QMS	[52,95,97]
9.	$Mg(BH_4)_2 \xrightarrow{290\ ^\circ C} MgH_2 + 2B + 3H_2 \xrightarrow{317\ ^\circ C} Mg + H_2$	TPD, ex-situ PXD	[42,43]
10.	α-$Mg(BH_4)_2 \xleftrightarrow{-4.5\ wt\%,\ >275^\circ C}$ amorphous phases, $BH_4^- \xrightarrow{-5\ wt\%}$ amorphous phases + B + BH_4^- + am.$MgB_4 \rightarrow 1/12\ MgB_{12}H_{12} + MgH_2 + MgB_4 \xrightarrow{-3\ wt\%} 1/12\ MgB_{12}H_{12}$ + Mg + $MgB_4 \xrightarrow{-2.5\ wt\%} MgB_2$	Ex-situ and in-situ PXD + MS, ^{11}B-SS-NMR, DSC, TPD in vacuum; first step is reversible	[98]
11.	$3Mg(BH_4)_2 \leftrightarrow Mg(B_3H_8)_2 + 2MgH_2 + 2H_2 \xrightarrow{>300\ ^\circ C} B_nH_{n+5}^-$, $B_{10}H_{10}^{2-}$, $B_{12}H_{12}^{2-}$, $B_nH_{n+3}^-$ $(3 < n < 12)$	First step is reversible at mild conditions; D_2O-NMR	[100,106]
12.	$BH_4^- \rightarrow B_2H_6^{2-} \rightarrow B_5H_9^{2-}$ or $B_5H_8^- \rightarrow B_{12}H_{12}^{2-}$	PXD, ^{11}B SS-NMR	[109]
13.	$2\ \alpha$-$Mg(BH_4)_2 \rightarrow 2\ MgB_2H_7 + H_2 \rightarrow 2\ MgB_2H_6 + H_2$ $3\ MgB_2H_6 \rightarrow 2\ MgBH_4 + MgB_4 + 5H_2$ $12MgBH_4 \rightarrow MgB_{12}H_{12} + 11MgH_2 + 7H_2$ $MgB_{12}H_{12} \rightarrow MgH_2 + 12B + 5H_2$ $MgH_2 + 2B \rightarrow MgB_2 + H_2$	DSC-TGA, PXD	[104]
14.	γ-$Mg(BH_4)_2 \xrightarrow{280-310\ ^\circ C}$ amorphous species/melt $\xrightarrow{310-370\ ^\circ C} MgH_2 \xrightarrow{340-570\ ^\circ C} Mg \xrightarrow{490-600\ ^\circ C} MgB_2$	In-situ and ex-situ PXD, FTIR, TPD	[57]
15.	γ-$Mg(BH_4)_2 \xrightarrow{215-330\ ^\circ C}$ amorphous species ($MgB_{12}H_{12}$ + other polyborane species) + $H_2 \xrightarrow{330-365\ ^\circ C} MgH_2 \xrightarrow{365-410\ ^\circ C} Mg + H_2$	In-situ PXD + TGA + MS ^{11}B SS-NMR	[54]
16.	am-$Mg(BH_4)_2 \xrightarrow{ca.\ 300\ ^\circ C} 1/6\ MgB_{12}H_{12} + 5/6\ MgH_2 + 13/6H_2 \xrightarrow{ca.\ 355\ ^\circ C} Mg(MgH_2) + 12\ B + 6H_2$; $MgH_2 \xrightarrow{ca.\ 355\ ^\circ C} Mg + H_2$	Ex-situ PXD, ^{11}B SS-NMR, TPD	[49]
17.	am-$Mg(BH_4)_2 \rightarrow Mg(B_xH_y)_n + H_2 \rightarrow Mg + B_2H_6 + H_2$	In-situ PXD, in-situ Raman	[63]
18.	$Mg(BH_4)_2 \xrightarrow{<300\ ^\circ C,\ dynamic\ vacuum} Mg(B_3H_8)_2 + (-[B_3H_7]-[B_nH_n]-) \xrightarrow{ca.\ 500\ ^\circ C} MgB_2$	DMSO-d_6-NMR, SS-NMR, FTIR	[105]
19.	(in vacuum) γ-$Mg(BH_4)_2 \xrightarrow{205-225\ ^\circ C} Mg(BH_4)_2 + MgH_2$ (am) + Mg–B–H (I) (possibly MgB_4H_{10}) $\xrightarrow{250\ ^\circ C} Mg(BH_4)_2 + MgH_2$ (am) + Mg–B–H (I) (possibly MgB_4H_{10}) $\xrightarrow{300\ ^\circ C}$ Mg (sublimated) + MgO + MgB_2 + Mg–B–H (II) $\xrightarrow{400\ ^\circ C}$ Mg (sublimated) + MgO + MgB_2 + Mg–B–H (III); (in H_2) γ-$Mg(BH_4)_2 \xrightarrow{205-225\ ^\circ C} Mg(BH_4)_2 + MgH_2$ (am) + Mg–B–H (I) (possibly MgB_4H_{10}) $\xrightarrow{250\ ^\circ C} Mg(BH_4)_2 + MgH_2$ (am) + Mg–B–H (I) (possibly MgB_4H_{10}) $\xrightarrow{300\ ^\circ C} MgH_2 + MgO + MgB_2$ + Mg–B–H (II) $\xrightarrow{400\ ^\circ C} Mg + MgO + MgB_2$ + Mg–B–H (III)	Ex-situ PXD, FTIR, UV–Vis, DFT	[59]

[a] Starting phase at RT *(the phase transitions are not shown)*; TPD – temperature-programmed desorption, SS-NMR – solid-state NMR; MAS-NMR – magic angle spinning NMR (≡SS-NMR); amorphous phases - $Mg_nB_xH_y$ either B_xH_y compounds; UV–Vis – ultraviolet–visible spectroscopy, FTIR – Fourier transformed infrared spectroscopy, MS – mass spectrometry, QMS – quadruple mass spectrometry, TPD – temperature-programmed desorption, DSC – differential scanning calorimetry, TG – termogravimetric methods.

impurities from the pores of γ-$Mg(BH_4)_2$ and/or sublimation of the sample for measurements in dynamic vacuum [59]. This conclusion is in agreement with the study [41] where the weight loss of as-received γ-$Mg(BH_4)_2$ and the sample treated with supercritical N_2 below 300 °C was compared. Such treatment was shown to clean the pores of the sample and reduce the weight loss below 200 °C (although it was still non-zero after cleaning). On the other hand, according to [59], one of the decomposition phases of $Mg(BH_4)_2$ (formed after 200 °C) contains boron fragments with characteristic IR vibrations at 770,748 and 695 cm^{-1}, respectively. Note that similar weak peaks can be observed in the spectra of ε- and β′-$Mg(BH_4)_2$ reported in this work (inset of Fig. 1b). These samples were obtained by heating γ-$Mg(BH_4)_2$ up to 175 and 212 °C (without any isothermal step) with the corresponding weight loss shown in Fig. 2a. Thus, it appears that some decomposition has already occurred together with the formation of the ε-$Mg(BH_4)_2$ below 175 °C. Therefore decomposition of γ-$Mg(BH_4)_2$ below 200 °C cannot be ruled out.

The overall decomposition reaction of $Mg(BH_4)_2$ can be described by simple pathways (Reactions 1–3 in Table 5). In early studies [32,94] it was shown by *in-situ* PXD that Mg was formed in small quantities together with MgH_2. Thus, Mg was not solely the decomposition product of MgH_2. Shortly later, it became obvious that the decomposition reaction follows a complex pathway with 5–6 steps and the formation of intermediate amorphous phases alongside with the crystalline reaction products (Table 5). The DSC data reported in Fig. 2a demonstrate at least four endothermic events in the 250–450 °C region. The ex-situ and in-situ PXD analyses, typically used to follow the reactions in complex hydrides [101–103], have been indicating amorphous intermediates in the ~280–320 °C region (step I on Fig. 2a), and some authors observed melting of $Mg(BH_4)_2$ [57,59]. The only crystalline magnesium boron hydride reaction intermediate MgB_2H_6 was found in Ref. [104] after a PCT experiment at 277 °C. Valuable information on amorphous phases can be drawn from NMR and vibrational spectroscopy studies. However, both techniques produce complex spectra with broad signals leaving the space for different interpretation. Some authors have been using D_2O-solution NMR in order to achieve high resolution signal [60,100], which could have affected the results due to the possible reaction of water with unstable borohydrides. Thus solid state (SS) NMR and solution NMR with D_2O and anhydrous solvents give contradictory results on the presence of $MgB_{12}H_{12}$ among the decomposition products (see Table 5). Yan et al. [105] suggested that the decomposition of $Mg(BH_4)_2$ occurs via polymerization process with $B_{12}H_{12}^{-}$ as a possible fragment of a larger boron hydride polymer. They conclude that this can explain the presence of $B_{12}H_{12}^{-}$ in D_2O solution where the Mg–B–H polymer disintegrates into various $B_nH_n^{-}$ monomers. The challenges of the NMR experimental approach and results interpretation were discussed in details in Ref. [57]. These authors pointed out that the decomposition intermediate below 300 °C, suggested as $Mg(B_3H_8)_2$ by Ref. [100] on basis of D_2O-solution NMR, might have been formed from the reaction between D_2O and boron hydride compounds, and that no signal of $B_3H_8^{2-}$ species had been detected by the SS-NMR. On the other hand, solution DMSO-d_6-NMR have also identified $(B_3H_8)^{-}$ as a possible reaction intermediate [105].

The IR and Raman spectroscopies also have been providing inconclusive results because of the rich boron hydride chemistry and unavailability of the spectra of all possible reference compounds [58–63]. Most of the reported IR and Raman spectra do not correspond straightforwardly to any of the known spectra of the reference compounds. However, these studies have not shown any clear evidence for the bridged B–H–B molecular species that could be characteristic for many MgB_xH_y compounds, including $Mg(B_3H_8)_2$. In Ref. [59] MgB_4H_{10} is suggested as the reaction intermediate on the basis of IR spectroscopic studies combined with DFT calculations. Note that both pathways yielding MgB_4H_{10} and $Mg(B_3H_8)_2$ (11 and 19 in Table 5) envisage the simultaneous formation of MgH_2. However, crystalline MgH_2 has been found to form at higher temperatures (most probably step II in Fig. 2a). While some authors [59,98] suggested the formation of amorphous MgH_2, Paskevicius et al. [57] noted that "no such phase has ever been observed previously for MgH_2".

Understanding the nature of amorphous intermediates is crucial in order to achieve reversibility of hydrogen desorption. The stable compounds such as $MgB_{12}H_{12}$ would lead to challenges with respect to reversibility in view of the high stability of the closed B_{12}-cage. On the other hand, the amorphous phases formed below 300 °C have proven to be partially reversible in much milder conditions than those described in Section Solvent-free chemistry [60–62,98,100,106,107]. Cycling of about 2 wt% of H_2 for three cycles was also recently demonstrated [62]. The desorption reaction was carried out at 0.3 MPa H_2 and 285 °C and yielded an amorphous phase, and the absorption reaction was possible at 12 MPa H_2. The PXD analysis of the partially decomposed $Mg(BH_4)_2$ did not show any crystalline MgH_2. Identifying the amorphous intermediates is still ongoing. This is crucial for improving hydrogen desorption and absorption in $Mg(BH_4)_2$.

Many experimental reports have shown that amorphous intermediates exist in each decomposition step until at least 450 °C [54,57,59,105]. Thus each step can comprise several competing reactions which can be affected by the reaction conditions and/or the sample history. For example, Hanada et al. noted that the decomposition pathway in H_2 was more spread out in temperature compared to the decomposition in He, and an additional desorption step appeared in the data with H_2 [94]. Kinetic modeling of intermediate decomposition reaction has indicated a complex pathway with possibly several competing reactions [61,62]. Formation of MgB_2 already after decomposition at 300 °C was observed for the sample synthetized via reactive ball-milling (pathway 16 in Table 5); although in the majority of the studies MgB_2 was found after the last decomposition step above 450 °C. These findings suggest that the experimental conditions and sample history can also influence the reaction pathways.

Kinetics and thermodynamics of decomposition reactions

Fig. 2b reports the E_a of each decomposition step (I–IV) for γ-$Mg(BH_4)_2$, obtained in this work. These values were obtained by applying Kissinger method to the DSC measurements at different heating rates [110]. The first step in our data has the highest kinetic barrier (E_a = 244 ± 17 kJ mol^{-1}), the other

values ranging between 139 and 157 kJ mol^{-1}. Interestingly, significantly lower E_a (99–55 kJ mol^{-1}) was reported for multi-step decomposition of α-$Mg(BH_4)_2$, also obtained from calorimetric measurements analyzed with the Kissinger method [104]. Fichtner et al. reported 311 ± 20 and 189 ± 15 kJ mol^{-1}, respectively, for the two-step decomposition reaction in $Mg(BH_4)_2$ [96], and Ibikunle at al. obtained only one value 155.2 kJ mol^{-1} [111]. Our E_a corresponding to the first decomposition step is higher than E_a reported for $LiBH_4$ (~60 kJ mol^{-1} [112]) and similar to $Ca(BH_4)_2$ (~225–280 kJ mol^{-1} [113]). It is worth noting that high kinetic barriers were suggest as the reason for the high T_{dec} of $Mg(BH_4)_2$ despite of the favorable thermodynamics predicted by the DFT [99].

An overview of thermodynamic data relevant for hydrogen storage properties of $Mg(BH_4)_2$ was recently published by Pinatel et al. [114], who also noted the inconsistency in the literature data. The authors have determined the relative stabilities of the α-, β-, and γ-polymorphs, calculated stable and metastable phase diagrams, and studied different dehydrogenation pathways of $Mg(BH_4)_2$. For the enthalpy of formation of $Mg(BH_4)_2$, the following reactions were considered:

$$Mg(BH_4)_2 \rightarrow Mg + 2B + 4H_2 \quad (1)$$

$$Mg(BH_4)_2 \rightarrow MgB_2 + 4H_2 \quad (2)$$

For reaction (1) the experimental value of ~170 kJ mol^{-1}, obtained via DSC method at 1 bar H_2, was reported [95]. The theoretical calculations resulted in 204 [19] and 277 kJ mol^{-1} [71]. For reaction (2), 152 kJ mol^{-1} has been calculated [19]. The enthalpy of the reaction

$$Mg(BH_4)_2 \rightarrow MgH_2 + 2B + 3H_2, \quad (3)$$

was found experimentally as 132 kJ mol^{-1} by DSC at 1 bar H_2 [95]; 171 kJ mol^{-1} [52] and 118 kJ mol^{-1} [43] by PCT measurements. The theoretical calculations resulted in 120 kJ mol^{-1} [114].

Effect of additives on hydrogen storage properties of $Mg(BH_4)_2$

Transition-metal (TM) additives have been shown to significantly improve the kinetics of hydrogen desorption and absorption in MgH_2 [115–117]. Titanium and other transition metals are crucial additives for the reversibility in several Al-based complex hydrides (alanates) and in particular $NaAlH_4$ [118–120]. The use of various TM-based additives has been extensively explored in order to enhance the hydrogen storage properties of different hydrides, including metal borohydrides (see for example [121–123] and refs. therein). It is envisioned that TM-additives can enhance reversible formation of a borohydride by forming heterogeneous nucleation sites, for example, CaB_6 in $Ca(BH_4)_2$ [124]. Elsewise the additives could affect breaking and formation of the B–H bonds similarly to the catalytic effects in organic hydrogenation and dehydrogenation reactions.

Several studies have shown a decrease in T_{dec} of different polymorphs and composites of $Mg(BH_4)_2$ with small quantities (~2 mol%) of TM additives, such as $NbCl_5$, NbF_5, $TiCl_3$, TiO_2, Ti–Nb, TiF_3, $ScCl_3$, $CoCl_2$, ZnF_2 [31,39,60,62,125–128]. This effect has mostly been investigated during the first hydrogen desorption, and only few of the studies have explored the effect of the additives on the rehydrogenation. Bardaji et al. [126] did not observe rehydrogenation of $Mg(BH_4)_2$ decomposed above 450 °C in the presence of Ti- and Nb-based additives. Newhouse et al. [39] were able to reform $Mg(BH_4)_2$ from its decomposition products in the presence of 5 mol% of TiF_3 and $ScCl_3$ under 90 MPa H_2, although rehydrogenation was also observed in the samples without additives. Ni-based additives were shown to improve hydrogen absorption (and desorption) kinetics in partially decomposed $Mg(BH_4)_2$ composites at moderate conditions (up to 12 MPa H_2 and 220–260 °C) [129]. Similarly, Co-based additives were found to enhance the decomposition kinetics and hamper rehydrogenation kinetics of γ-$Mg(BH_4)_2$ in the first cycle and thus stabilizing the decomposition products [62]. These effects were shown to diminish upon 3 cycles.

The lowering of T_{dec} by using additives appears to be related to chemical reactions between the additive and $Mg(BH_4)_2$. In spite of their stability, even TM-borides were shown to lose the long-range order when heated together with $Mg(BH_4)_2$ [60,62]. $CoCl_2$ added to $LiBH_4 + Mg(BH_4)_2$ composite reacted to form $LiMgCl_3$ [127]. $TiCl_3$ in $Mg(BH_4)_2$ converted to $Ti_xMg_{1-3x/2}(BH_4)_2$ (x = 0–0.67) after ball-milling, and subsequently to TiB_2 during the first dehydrogenation step (100–150 °C) [130]. Ti^{4+} in TiO_2 was reduced to lower oxidation state at the temperature around the main dehydrogenation peak of $Mg(BH_4)_2$ (350 °C). Ni- and Co-based additives in γ-$Mg(BH_4)_2$ formed new compounds with amorphous boride-like structure during $Mg(BH_4)_2$ decomposition [60,62]. These in-situ formed compounds were suggested to be responsible for the improved hydrogen kinetics. However, in a recent study [62] these effects were found to diminish with cycling. The combined in-situ X-ray and Raman study showed that the added CoF_2 and $CoCl_2$ affected the phase-transition T in γ-$Mg(BH_4)_2$ and reacted with the borohydride matrix forming metal clusters rather than CoB_x species upon reduction. In case of $CoCl_2$ additive, TEM observations suggested that some of the Co was incorporated into the hydride surfaces already after ball-milling [58].

In summary, the effects of the additives in borohydrides could be attributed to chemical reactions between the two and possibly to the ball-milling process used to disperse the additives. In fact, mere mechanical milling of $Mg(BH_4)_2$ was shown to significantly improve the kinetics of H_2 desorption and absorption in γ-$Mg(BH_4)_2$ [58]. On the other hand, it has also been found that ball-milling did not have any noteworthy effect on the decomposition of β-$Mg(BH_4)_2$ [31].

Other approaches for destabilization of $Mg(BH_4)_2$

Other approaches to enhance hydrogen storage properties of borohydrides have been the dispersion in a porous matrix [88,96,131,132,134–141] and/or preparation of reactive hydride

composites (RHCs) [133,141–149]. The first approach aims at profiting from the modification of thermodynamics and kinetics because of surface effects [134], whereas RHCs aims at modifying the thermodynamics properties by reducing the overall ΔH of the reaction. Several groups have attempted to confine or directly synthetize $Mg(BH_4)_2$ in high SSA porous matrix such as pre-treated nanoporous and mesoporous carbon [96,131,135,136], carbon aerogel [137,141], milled graphite [138], active carbon fibers [139], or porous silica [139], etc. The most promising achievements showed a nearly two-fold decrease in the E_a of the first decomposition step [96], or shifts of the T_{dec} by more than 100 °C [135,138]. Ingleson et al. [140] reported the synthesis of the first porous metal-organic framework (MOF) based on $Mg(BH_4)_2$ and pyrazine. The BH_4^- ions in the compound decomposed at only 140 °C, however with hydroboration of pyrazine rather than H_2 release. Nanoconfinement of the $0.55LiBH_4$–$0.45\ Mg(BH_4)_2$ RHC in high surface area carbon aerogel was shown to facilitate hydrogen release and uptake comparing to the bulk sample [141]. Adding $Mg(BH_4)_2$ to $Mn(BH_4)_2$ which is known to decompose via release of undesirable byproduct B_2H_6 was shown to promote instead the release of H_2 from the composite [144]. Similarly, the $Mg(BH_4)_2$–$ZnCl_2$ mixtures, which upon ball-milling can form $Zn(BH_4)_2$ that decomposes with the release of B_2H_6, were shown to desorb pure hydrogen above 125 °C for almost all composite $Mg(BH_4)_2$:$ZnCl_2$ ratios [147,149].

It can be noted that the best results, such as dramatic decrease in T_{dec} of $Mg(BH_4)_2$ and other borohydrides, was observed for composites where several destabilization approaches were combined, for example, using TM-additives and dispersion in highly porous media [131,132] or combination of TM-additives with electron-rich compound, such as metal hydrides or nitrogen-containing hydrides [133].

$Mg(BH_4)_2$ for applications in batteries

Development of batteries with improved energy density and cost per energy compared to the existing commercially available Li-ion batteries is envisaged to decrease cost and increase range of electric vehicles [20]. Post-lithium-ion battery technologies were suggested as a promising pathway to achieve these goals [20,150,151]. Since the discovery of the lithium fast-ionic conductivity in $LiBH_4$ [152], borohydrides have been the subject of thorough studies for electrochemical energy storage systems, including all solid-state batteries [153–156]. As soon as the feasibility of a secondary magnesium battery was demonstrated [157], the interest in developing Mg-based ionic transporters has increased significantly. Mg holds better volumetric capacity than Li metal (3833 mAh cm^{-3} compared to 2036 mAh cm^{-3}), has similarly high negative reduction potential (−2.4 V), do not appear to suffer from the dendrite formation to the same degree as lithium [158,159], is more stable towards air and more abundant. In fact, most of the research efforts on rechargeable multivalent batteries have focused on the non-aqueous magnesium electrochemistry [20].

In the batteries research, $Mg(BH_4)_2$ has been mainly considered as a liquid electrolyte for Mg-batteries [20,160–165]. Electrodeposition of Mg on Cu cathodes from $Mg(BH_4)_2$ formed in situ by reaction of MgBr and $LiBH_4$ was demonstrated as early as 1957 [160], however it was accompanied by co-deposition of boron. Mohtadi et al. have demonstrated the solvation of Mg(BH4)2 in THF or DME to use as electrolyte that enable the reversible Mg deposition and stripping in the presence of a standard Chevrel phase cathode [161,166]. The electrochemical performance of $Mg(BH_4)_2$ in DME was better than in THF, and the deposited magnesium was not contaminated by boron. The addition of $LiBH_4$ was shown to increase the current densities by several orders of magnitude and the coulombic efficiencies up to 94%. Using cyclic voltammetry, the reversibility of Mg deposition/dissociation was demonstrated using $Mg(BH_4)_2$ in different organic solvents (THF, DME, tetraglyme, diglyme) [162]. A complete secondary magnesium battery has been proposed, in which $Mg(BH_4)_2$ and TiO_2 were used as liquid electrolyte (0.5 M $Mg(BH_4)_2$/1.5 M $LiBH_4$ in tetraglyme solvent) and as cathode [163], respectively. The authors demonstrated that the charge/discharge capacity of the battery had been fairly preserved at the value of ~140 mAh g^{-1} after 80 cycles. Chang et al. [164] studied electrochemical deposition of Mg using the electrolyte 0.1 M $Mg(BH_4)_2$/1.5 M $LiBH_4$ in diglyme solution and Pt ultramicroelectrode. The presence of Li ions was shown to lead to the co-deposition of Mg–Li solid solution in which the composition depended on the potential and mass transfer. The exceptional performance suitable for batteries was attributed to the co-intercalation of Li and Mg ions [164]. The reversible cycling of $Mg(BH_4)_2$ amorphous phase in a Li half-cell was reported with poor reversible capacity [165]. However, the authors did not provide experimental evidence on the assumed theoretical reaction pathways during charge and discharge. Unfortunately, the oxidative stability of $Mg(BH_4)_2$ has been reported similar to that of Grignard solutions [20].

One of the main reasons to utilize borohydrides in batteries was the interesting solid-state conductivity of more than 1×10^{-3} S/cm over 117 °C reported for solid $LiBH_4$ [152]. Solid-state electrolytes would have decreased the rate of parasitic reactions at the electrolyte/electrode interface improving durability and safety. The ionic conductivity of Mg in the HT-$Mg(BH_4)_2$ phase was studied by first-principles molecular dynamics (FPMD) [156]. The authors noted that in the HT-$Mg(BH_4)_2$ Mg^{2+} is located in the relatively small tetrahedral cage made up by four BH_4^- ions. By contrast, in the HT-$LiBH_4$ and $Na_2(BH_4)(NH_2)$ phases, the hexagonal and octahedral coordination of the cations result in the fast Li^+ and Na^+ ionic conductivities. In HT-$Mg(BH_4)_2$, on the contrary, because of the close proximity of the anions, Mg^{2+} cannot diffuse out of the cage, resulting in zero net ionic diffusion, according to the FPMD simulations. No experimental studies on the Mg conductivity in solid $Mg(BH_4)_2$ has to the best of our knowledge been reported yet.

Summary

$Mg(BH_4)_2$ is one of the most interesting borohydrides in view of the unique properties and potential for applications. The variety and complexity of structures is of a great interest for both experimentalists and theoreticians. High hydrogen densities and low enthalpy of formation reaction are important for hydrogen storage applications. Experiments also indicate that T_{dec} of $Mg(BH_4)_2$ is the lowest among the Group I and II

borohydrides, and upon decomposition the compound releases mostly pure H_2 with negligible if any amounts of B_2H_6. However, hydrogen desorption kinetics of $Mg(BH_4)_2$ presents a challenge, the E_a for the first decomposition step being higher than that of $LiBH_4$ and $Ca(BH_4)_2$. Hydrogen re-absorption requires impractically high H_2 pressures, temperatures and reaction times. Partial reversibility and cycling of H_2 for 3 cycles in relatively mild conditions has been demonstrated. However the amount of H_2 recharged at those conditions was only about ~2.5 wt%, and thus impractically low. One of the keys in improving the H_2 release kinetics is to understand the complex multistep decomposition pathway of $Mg(BH_4)_2$. As shown in this review, several alternative decomposition pathways have been proposed in the literature. By understanding the details of the decomposition reaction, it might be possible to affect it by choosing a proper additive. So far using TM-based additives has not demonstrated the desirable effects. In several cases, T_{dec} for the first decomposition was significantly reduced, but data on the effect on H_2 cycling of $Mg(BH_4)_2$ with various additives are still very limited. The only published study with several cycles with Co-additives in $Mg(BH_4)_2$ have shown that the effects demonstrated in the first cycle diminish towards the third cycle, and therefore prompting for looking into other additives. More promising results might be achieved with application of other strategies, such as preparation of the reactive hydride composites with $Mg(BH_4)_2$ and/or nanoconfinement. The unique porous phase of γ-$Mg(BH_4)_2$ may open new application directions where surface effects are dominant. The research exploring the potential application of $Mg(BH_4)_2$ in batteries is only at an initial stage.

Acknowledgments

This work was financed by the European Fuel Cells and Hydrogen Joint Undertaking (http://www.fch-ju.eu) under collaborative project "BOR4STORE" (Grant agreement no.: N° 303428). Partial funding from FP7 COST-action MP1103 "Nanostructured materials for solid-state hydrogen storage" is gratefully acknowledged.

REFERENCES

[1] López González E, Isorna Llerena F, Silva Pérez M, Rosa Iglesias F, Guerra Macho J. Energy evaluation of a solar hydrogen storage facility: comparison with other electrical energy storage technologies. Int J Hydrogen Energy 2015;40:5518–25.
[2] Ross DK. Hydrogen storage: the major technological barrier to the development of hydrogen fuel cell cars. Vacuum 2006;80:1084–9.
[3] Hirscher M. Handbook of hydrogen storage new materials for future energy storage. Weinheim Wiley-VCH-Verl; 2010.
[4] Ronnebro E, Majzoub EH, editors. Metal hydrides for clean enegy applications. CAMBRIDGE University Press; 2013.
[5] Marrero-Alfonso EY, Beaird AM, Davis TA, Matthews MA. Hydrogen generation from chemical hydrides. Ind Eng Chem Res 2009;48:3703–12.
[6] Umegaki T, Yan J-M, Zhang X-B, Shioyama H, Kuriyama N, Xu Q. Boron- and nitrogen-based chemical hydrogen storage materials. Int J Hydrogen Energy 2009;34:2303–11.
[7] Wang J, Li HW, Chen P. Amides and borohydrides for high capacity solid-state hydrogen storage - materials design and kinetics improvement. MRS Bull 2013;38:480–7.
[8] Weidenthaler C, Felderhoff M. Solid-state hydrogen storage for mobile applications: quo vadis? Energy Environ Sci 2011;4:2495–502.
[9] Solid hydrogen storage. http://www.mcphy.com/en/products/solid-hydrogen-storage/ [accessed 10.12.15].
[10] Hydrexia's Patented Hydrogen Storage Technology. http://hydrexia.com/hydrexia-hydrogen-storage-technology/ [accessed 10.12.15].
[11] Energy OoEEaR. Hydrogen Storage. http://energy.gov/eere/fuelcells/hydrogen-storage [accessed 10.12.15].
[12] Saldan I. A prospect for $LiBH_4$ as on-board hydrogen storage. Centr Eur J Chem 2011;9:761–75.
[13] Züttel A, Rentsch S, Fischer P, Wenger P, Sudan P, Mauron P, et al. Hydrogen storage properties of $LiBH_4$. J Alloys Compd 2003;356:515–20.
[14] George L, Saxena SK. Structural stability of metal hydrides, alanates and borohydrides of alkali and alkali- earth elements: a review. Int J Hydrogen Energy 2010;35:5454–70.
[15] Filinchuk Y, Richter B, Jensen TR, Dmitriev V, Chernyshov D, Hagemann H. Porous and dense magnesium borohydride frameworks: synthesis, stability, and reversible absorption of guest species. Angew Chem Int Ed 2011;50:11162–6.
[16] Richter B, Ravnsbæk BD, Tumanov N, Filinchuk Y, Jensen RT. Manganese borohydride; synthesis and characterization. Dalton Trans 2015;44(9):3988–96.
[17] Ban V, Solonínin AV, Skripov AV, Hadermann J, Abakumov A, Filinchuk Y. Pressure-collapsed amorphous $Mg(BH_4)_2$: an ultradense complex hydride showing a reversible transition to the porous framework. J Phys Chem C 2014;118:23402–8.
[18] Ozolins V, Majzoub EH, Wolverton C. First-principles prediction of a ground state crystal structure of magnesium borohydride. Phys Rev Lett 2008:100.
[19] van Setten MJ, de Wijs GA, Fichtner M, Brocks G. A density functional study of alpha-$Mg(BH_4)_2$. Chem Mater 2008;20:4952–6.
[20] Muldoon J, Bucur CB, Gregory T. Quest for nonaqueous multivalent secondary batteries: magnesium and beyond. Chem Rev 2014;114:11683–720.
[21] Stasinevich DS, Egorenko GA. Thermal study of alkali-metals and magensium borohydride at pressures below 10 atm [ТерМографическое исследование борогидридов щелочных Металлов и Магния при давлении до 10 атМ]. Zh Neorg Khim 1968;13:654–8.
[22] Plesek J, Hermanek S. Chemistry of boranes. IV. On preparation, properties, and behavior towards Lewis bases of magnesium borohydride. Collect Czech Chem Commun 1966;31:3845–58.
[23] Bremer M, Linti G, Noth H, Thomann-Albach M, Wagner G. Metal tetrahydroborates and tetrahydroborato metalates. 30 1 solvates of alcoholato-, phenolato-, and bis(trimethylsilyl)amido-magnesium tetrahydroborates XMgBH4(L-n). Z Anorg Allg Chem 2005;631:683–97.
[24] Bremer M, Noth H, Warchhold M. Metal tetrahydroborates and tetrahydroborato metallates, 28: Part 27: the structure of some amine solvates of magnesium bis(tetrahydroborate) and DFT calculations on solvates of lithium tetrahydroborate. Eur J Inorg Chem 2003:111–9.

[25] Kuznetsov VA, Dymova TN. Standard enthalpies and Geebs free energy of formation of several complex hydrides [Оценка стандартных энтальпий и изобарных потенциалов образования некоторых коМплексных гидридов]. Russ Chem Bull 1971:260–4.

[26] Konoplev VN, Maltseva NN, Khain VS. Tetrahydroborates of metals of II-A-Group. Koord Khim 1992;18:1143–66.

[27] Wiberg VE, Bauer R. Zur Kenntnis eines Magneshim-borwasserstoffs $Mg(BH_4)_2$. Z Naturforsch B 1950;5:397.

[28] Köster R. Neue Herstellungsmethoden für Metallborhydride. Angew Chem 1957;69:94.

[29] Nakamori Y, Miwa K, Ninomiya A, Li H, Ohba N, Towata S-i, et al. Correlation between thermodynamical stabilities of metal borohydrides and cation electronegativites: first-principles calculations and experiments. Phys Rev B 2006;74:045126.

[30] Chlopek K, Frommen C, Leon A, Zabara O, Fichtner M. Synthesis and properties of magnesium tetrahydroborate, $Mg(BH_4)_2$. J Mater Chem 2007;17:3496–503.

[31] Li HW, Kikuchi K, Nakamori Y, Miwa K, Towata S, Orimo S. Effects of ball milling and additives on dehydriding behaviors of well-crystallized $Mg(BH_4)_2$. Scr Mater 2007;57:679–82.

[32] Riktor MD, Sørby MH, Chlopek K, Fichtner M, Buchter F, Züttel A, et al. In situ synchrotron diffraction studies of phase transitions and thermal decomposition of $Mg(BH_4)_2$ and $Ca(BH_4)_2$. J Mater Chem 2007;17:4939–42.

[33] Zanella P, Crociani L, Masciocchi N, Giunchi G. Facile high-yield synthesis of pure, crystalline $Mg(BH_4)_2$. Inorg Chem 2007;46:9039–41.

[34] Hagemann H, Cerny R. Synthetic approaches to inorganic borohydrides. Dalton Trans 2010;39:6006–12.

[35] Soloveichik GL, Andrus M, Gao Y, Zhao JC, Kniajanski S. Magnesium borohydride as a hydrogen storage material: synthesis of unsolvated $Mg(BH_4)_2$. Int J Hydrogen Energy 2009;34:2144–52.

[36] Cerny R, Filinchuk Y, Hagemann H, Yvon K. Magnesium borohydride: synthesis and crystal structure. Angew Chem Int Ed 2007;46:5765–7.

[37] Her J-H, Stephens PW, Gao Y, Soloveichik GL, Rijssenbeek J, Andrus M, et al. Structure of unsolvated magnesium borohydride $Mg(BH_4)_2$. Acta Crystallogr Sect B Struct Sci 2007;63:561–8.

[38] Filinchuk Y, Cerny R, Hagemann H. Insight into $Mg(BH_4)_2$ with synchrotron X-ray diffraction: structure revision, crystal chemistry, and anomalous thermal expansion. Chem Mater 2009;21:925–33.

[39] Newhouse RJ, Stavila V, Hwang S-J, Klebanoff LE, Zhang JZ. Reversibility and improved hydrogen release of magnesium borohydride. J Phys Chem C 2010;114:5224–32.

[40] Bateni A, Scherpe S, Acar S, Somer M, International JP. Novel approach for synthesis of magnesium borohydride, $Mg(BH_4)_2$. In: Whec 2012 Conference Proceedings - 19th World Hydrogen Energy Conference; 2012. p. 26–33.

[41] Stadie NP, Callini E, Richter B, Jensen TR, Borgschulte A, Züttel A. Supercritical N-2 processing as a route to the clean dehydrogenation of porous $Mg(BH_4)_2$. J Am Chem Soc 2014;136:8181–4.

[42] Matsunaga T, Buchter F, Miwa K, Towata S, Orimo S, Züttel A. Magnesium borohydride: a new hydrogen storage material. Renew Energy 2008;33:193–6.

[43] Matsunaga T, Buchter F, Mauron P, Bielman A, Nakamori Y, Orimo S, et al. Hydrogen storage properties of $Mg(BH_4)_2$. J Alloys Compd 2008;459:583–8.

[44] Varin RA, Chiu C, Wronski ZS. Mechano-chemical activation synthesis (MCAS) of disordered $Mg(BH_4)_2$ using NaBH4. J Alloys Compd 2008;462:201–8.

[45] Zhang ZG, Luo FP, Wang H, Liu JW, Zhu M. Direct synthesis and hydrogen storage characteristics of Mg-B-H compounds. Int J Hydrogen Energy 2012;37:926–31.

[46] Zhang ZG, Zhang SF, Wang H, Liu JW, Zhu M. Feasibility study of the direct synthesis of $Mg(BH_4)_2$ complex hydrides by mechanical milling. J Alloys Compd 2010;505:717–21.

[47] Severa G, Rönnebro E, Jensen CM. Direct hydrogenation of magnesium boride to magnesium borohydride: demonstration of > 11 weight percent reversible hydrogen storage. Chem Commun 2010;46:421–3.

[48] Pistidda C, Garroni S, Dolci F, Bardaji EG, Khandelwal A, Nolis P, et al. Synthesis of amorphous $Mg(BH_4)_2$ from MgB2 and H-2 at room temperature. J Alloys Compd 2010;508:212–5.

[49] Gupta S, Hlova IZ, Kobayashi T, Denys RV, Chen F, Zavaliy IY, et al. Facile synthesis and regeneration of $Mg(BH_4)_2$ by high energy reactive ball milling of MgB2. Chem Commun 2013;49:828–30.

[50] Kaya S, Guru M, Ar I. Synthesis of magnesium borohydride from its elements and usage in the hydrogen cycle. Energy Sources Part A Recovery Util Environ Eff 2011;33:2157–70.

[51] Pitt MP, Webb CJ, Paskevicius M, Sheptyakov D, Buckley CE, Gray EM. In Situ neutron diffraction study of the deuteration of isotopic (MgB2)-B-11. J Phys Chem C 2011;115:22669–79.

[52] Li HW, Kikuchi K, Nakamori Y, Ohba N, Miwa K, Towata S, et al. Dehydriding and rehydriding processes of well-crystallized $Mg(BH_4)_2$ accompanying with formation of intermediate compounds. Acta Mater 2008;56:1342–7.

[53] Zhang ZG, Wang H, Liu JW, Zhu M. Synthesis and hydrogen storage characteristics of Mg-B-H compounds by a gas-solid reaction. Int J Hydrogen Energy 2013;38:5309–15.

[54] David WIF, Callear SK, Jones MO, Aeberhard PC, Culligan SD, Pohl AH, et al. The structure, thermal properties and phase transformations of the cubic polymorph of magnesium tetrahydroborate. PCCP 2012;14:11800–7.

[55] George L, Drozd V, Saxena SK, Bardaji EG, Fichtner M. Structural phase transitions of $Mg(BH_4)_2$ under pressure. J Phys Chem C 2009;113:486–92.

[56] Cerny R, Penin N, Hagemann H, Filinchuk Y. The first crystallographic and spectroscopic characterization of a 3d-metal borohydride: $Mn(BH_4)_2$. J Phys Chem C 2009;113:9003–7.

[57] Paskevicius M, Pitt MP, Webb CJ, Sheppard DA, Filso U, Gray EM, et al. In-situ X-ray diffraction study of gamma-$Mg(BH_4)_2$ decomposition. J Phys Chem C 2012;116:15231–40.

[58] Zavorotynska O, Deledda S, Vitillo J, Saldan I, Guzik M, Baricco M, et al. Combined X-ray and Raman studies on the effect of cobalt additives on the decomposition of magnesium borohydride. Energies 2015;8:9173.

[59] Vitillo JG, Bordiga S, Baricco M. Spectroscopic and structural characterization of Thermal decomposition of γ-$Mg(BH_4)_2$: dynamic vacuum versus H_2 atmosphere. J Phys Chem C 2015;119:25340–51.

[60] Saldan I, Hino S, Humphries TD, Zavorotynska O, Chong M, Jensen CM, et al. Structural changes observed during the reversible hydrogenation of $Mg(BH_4)_2$ with Ni-based additives. J Phys Chem C 2014;118:23376–84.

[61] Zavorotynska O, Deledda S, Hauback B. Kinetics studies of the reversible partial decomposition reaction in $Mg(BH_4)_2$. Int J Hydrogen Energy Feb 2016. Proceedings of the mESC-IS 2015.

[62] Zavorotynska O, Saldan I, Hino S, Humphries TD, Deledda S, Hauback BC. Hydrogen cycling in gamma-$Mg(BH_4)_2$ with cobalt-based additives. J Mater Chem A 2015;3:6592–602.

[63] Guo S, Chan HYL, Reed D, Book D. Investigation of dehydrogenation processes in disordered gamma-$Mg(BH_4)_2$. J Alloys Compd 2013;580:S296–300.
[64] Stadie NP, Callini E, Mauron P, Borgschulte A, Züttel A. Supercritical nitrogen processing for the purification of reactive porous materials. J Vis Exp. 2015;(99):e52817. http://dx.doi.org/10.3791/52817.
[65] Vitillo JG, Groppo E, Bardaji EG, Baricco M, Bordiga S. Fast carbon dioxide recycling by reaction with gamma-$Mg(BH_4)_2$. PCCP 2014;16:22482–6.
[66] Zavorotynska O, Deledda S, Li G, Matsuo M, Orimo S-i, Hauback BC. Isotopic exchange in porous and dense magnesium borohydride. Angew Chem Int Ed 2015;54:10592–5.
[67] Dai B, Sholl DS, Johnson JK. First-principles study of experimental and hypothetical $Mg(BH_4)_2$ crystal structures. J Phys Chem C 2008;112:4391–5.
[68] Zhou X-F, Qian Q-R, Zhou J, Xu B, Tian Y, Wang H-T. Crystal structure and stability of magnesium borohydride from first principles. Phys Rev B 2009:79.
[69] Vajeeston P, Ravindran P, Kjekshus A, Fjellvåg H. High hydrogen content complex hydrides: a density-functional study. Appl Phys Lett 2006;89:071906.
[70] Voss J, Hummelshøj JS, Łodziana Z, Vegge T. Structural stability and decomposition of Mg(BH 4) 2 isomorphs—an ab initio free energy study. J Phys Condens Matter 2009;21:012203.
[71] Caputo R, Tekin A, Sikora W, Züttel A. First-principles determination of the ground-state structure of $Mg(BH_4)_2$. Chem Phys Lett 2009;480:203–9.
[72] Bil A, Kolb B, Atkinson R, Pettifor DG, Thonhauser T, Kolmogorov AN. van der Waals interactions in the ground state of $Mg(BH_4)_2$ from density functional theory. Phys Rev B 2011:83.
[73] Zhou X-F, Oganov AR, Qian G-R, Zhu Q. First-principles determination of the structure of magnesium borohydride. Phys Rev Lett 2012:109.
[74] Fan J, Bao K, Duan D-F, Wang L-C, Liu B-B, Cui T. High volumetric hydrogen density phases of magnesium borohydride at high-pressure: a first-principles study. Chin Phys B 2012:21.
[75] Fan J, Duan D, Jin X, Bao K, Liu B, Cui T. Structure determination of ultra dense magnesium borohydride: a first-principles study. J Chem Phys 2013:138.
[76] Lodziana Z, van Setten MJ. Binding in alkali and alkaline-earth tetrahydroborates: special position of magnesium tetrahydroborate. Phys Rev B 2010:81.
[77] Parker SF. Spectroscopy and bonding in ternary metal hydride complexes-Potential hydrogen storage media. Coord Chem Rev 2010;254:215–34.
[78] Renaudin G, Gomes S, Hagemann H, Keller L, Yvon K. Structural and spectroscopic studies on the alkali borohydrides MBH4 (M = Na, K, Rb, Cs). J Alloys Compd 2004;375:98–106.
[79] Carbonniere P, Hagemann H. Fermi resonances of borohydrides in a crystalline environment of alkali metals. J Phys Chem A 2006;110:9927–33.
[80] Zavorotynska O, Corno M, Damin A, Spoto G, Ugliengo P, Baricco M. Vibrational properties of MBH4 and MBF4 crystals (M = Li, Na, K): a combined DFT, infrared, and Raman study. J Phys Chem C 2011;115:18890–900.
[81] Hagemann H, Filinchuk Y, Chernyshov D, van Beek W. Lattice anharmonicity and structural evolution of LiBH4: an insight from Raman and X-ray diffraction experiments. Phase Transitions 2009;82:344–55.
[82] Zavorotynska O, Corno M, Pinatel E, Rude LH, Ugliengo P, Jensen TR, et al. Theoretical and experimental study of $LiBH_4$-LiCl solid solution. Crystals 2012;2:144–58.
[83] Fateley WG, Dollish FR, McDevitt T, Bentley FF. Infrared and Raman selection rules for molecular and lattice vibrations: the correlation method. New York: Wiley-Interscience; 1972.
[84] Gebert F, Willenberg B, van Setten MJ, Bardaji EG, Roehm E, Fichtner M, et al. Polarization-dependent Raman spectroscopy of LiBH4 single crystals and $Mg(BH_4)_2$ powders. J Raman Spectrosc 2011;42:1796–801.
[85] Giannasi A, Colognesi D, Ulivi L, Zoppi M, Ramirez-Cuesta AJ, Bardaji EG, et al. High resolution Raman and neutron investigation of $Mg(BH_4)_2$ in an extensive temperature range. J Phys Chem A 2010;114:2788–93.
[86] Hagemann H, D'Anna V, Rapin J-P, Cerny R, Filinchuk Y, Kim KC, et al. New fundamental experimental studies on alpha-$Mg(BH_4)_2$ and other borohydrides. J Alloys Compd 2011;509:S688–90.
[87] Zavorotynska O, Li G, Matsuo M, Deledda S, Orimo S, Hauback B. In-situ Raman Study of H → D exchange in γ-$Mg(BH_4)_2$. In: Gordon Research Conference on Metal-hydrogen systems. Eaton (MA), USA; 2015 [poster presentation].
[88] Shane DT, Rayhel LH, Huang Z, Zhao J-C, Tang X, Stavila V, et al. Comprehensive NMR study of magnesium borohydride. J Phys Chem C 2011;115:3172–7.
[89] Skripov AV, Soloninin AV, Babanova OA, Hagemann H, Filinchuk Y. Nuclear magnetic resonance study of reorientational motion in alpha-$Mg(BH_4)_2$. J Phys Chem C 2010;114:12370–4.
[90] Soloninin AV, Babanova OA, Skripov AV, Hagemann H, Richter B, Jensen TR, et al. NMR study of reorientational motion in alkaline-earth borohydrides: beta and gamma phases of $Mg(BH_4)_2$ and alpha and beta phases of $Ca(BH_4)_2$. J Phys Chem C 2012;116:4913–20.
[91] Eagles M, Sun B, Richter B, Jensen TR, Filinchuk Y, Conradi MS. NMR investigation of nanoporous gamma-$Mg(BH_4)_2$ and its thermally induced phase changes. J Phys Chem C 2012;116:13033–7.
[92] Hydrogen storage. US Department of Energy.
[93] Li H-W, Kikuchi K, Sato T, Nakamori Y, Ohba N, Aoki M, et al. Synthesis and hydrogen storage properties of a single-phase magnesium borohydride $Mg(BH_4)_2$. Mater Trans 2008;49:2224–8.
[94] Hanada N, Chlopek K, Frommen C, Lohstroh W, Fichtner M. Thermal decomposition of $Mg(BH_4)_2$ under He flow and H2 pressure. J Mater Chem 2008;18:2611–4.
[95] Yan Y, Li H-W, Nakamori Y, Ohba N, Miwa K, Towata S-i, et al. Differential scanning calorimetry measurements of magnesium borohydride $Mg(BH_4)_2$. Mater Trans 2008;49:2751–2.
[96] Fichtner M, Zhao-Karger Z, Hu J, Roth A, Weidler P. The kinetic properties of $Mg(BH_4)_2$ infiltrated in activated carbon. Nanotechnology 2009:20.
[97] Li HW, Miwa K, Ohba N, Fujita T, Sato T, Yan Y, et al. Formation of an intermediate compound with a B12H12 cluster: experimental and theoretical studies on magnesium borohydride $Mg(BH_4)_2$. Nanotechnology 2009:20.
[98] Soloveichik GL, Gao Y, Rijssenbeek J, Andrus M, Kniajanski S, Bowman Jr RC, et al. Magnesium borohydride as a hydrogen storage material: properties and dehydrogenation pathway of unsolvated $Mg(BH_4)_2$. Int J Hydrogen Energy 2009;34:916–28.
[99] van Setten MJ, Lohstroh W, Fichtner M. A new phase in the decomposition of $Mg(BH_4)_2$: first-principles simulated annealing. J Mater Chem 2009;19:7081–7.
[100] Chong M, Karkamkar A, Autrey T, Orimo S-i, Jalisatgi S, Jensen CM. Reversible dehydrogenation of magnesium borohydride to magnesium triborane in the solid state

under moderate conditions. Chem Commun 2011;47:1330–2.
[101] Filinchuk Y, Chernyshov D, Dmitriev V. Light metal borohydrides: crystal structures and beyond. Z Kristallogr 2008;223:649–59.
[102] Ravnsbæk DB, Filinchuk Y, Cerny R, Jensen TR. Powder diffraction methods for studies of borohydride-based energy storage materials. Z Kristallogr 2010;225:557–69.
[103] Cerny R, Filinchuk Y. Complex inorganic structures from powder diffraction: case of tetrahydroborates of light metals. Z Kristallogr 2011;226:882–91.
[104] Yang J, Zhang X, Zheng J, Song P, Li X. Decomposition pathway of $Mg(BH_4)_2$ under pressure: metastable phases and thermodynamic parameters. Scr Mater 2011;64:225–8.
[105] Yan Y, Remhof A, Rentsch D, Züttel A. The role of MgB12H12 in the hydrogen desorption process of $Mg(BH_4)_2$. Chem Commun 2015;51:700–2.
[106] Chong M, Matsuo M, Orimo S-i, Autrey T, Jensen CM. Selective reversible hydrogenation of $Mg(B_3H_8)_2/MgH_2$ to $Mg(BH_4)_2$: pathway to reversible borane-based hydrogen storage? Inorg Chem 2015;54:4120–5.
[107] Saldan I, Frommen C, Llamas-Jansa I, Kalantzopoulos GN, Hino S, Arstad B, et al. Hydrogen storage properties of gamma-$Mg(BH_4)_2$ modified by MoO_3 and TiO_2. Int J Hydrogen Energy 2015;40:12286–93.
[108] Hwang S-J, Bowman Jr RC, Reiter JW, Rijssenbeek J, Soloveichik GL, Zhao J-C, et al. NMR confirmation for formation of $[B_{12}H_{12}]^{2-}$ complexes during hydrogen desorption from metal borohydrides. J Phys Chem C 2008;112:3164–9.
[109] Yan Y, Li H-W, Maekawa H, Aoki M, Noritake T, Matsumoto M, et al. Formation process of $[B_{12}H_{12}]^{2-}$ from BH_4^- during the dehydrogenation reaction of $Mg(BH_4)_2$. Mater Trans 2011;52:1443–6.
[110] Kissinger HE. Reaction kinetics in differential Thermal analysis. Anal Chem 1957;29:1702–6.
[111] Ibikunle AA, Goudy AJ. Kinetics and modeling study of a $Mg(BH_4)_2/Ca(BH_4)_2$ destabilized system. Int J Hydrogen Energy 2012;37:12420–4.
[112] Pendolino F, Mauron P, Borgschulte A, Zuettel A. Effect of Boron on the activation energy of the decomposition of $LiBH_4$. J Phys Chem C 2009;113:17231–4.
[113] Mao J, Guo Z, Poh CK, Ranjbar A, Guo Y, Yu X, et al. Study on the dehydrogenation kinetics and thermodynamics of $Ca(BH_4)_2$. J Alloys Compd 2010;500:200–5.
[114] Pinatel ER, Albanese E, Civalleri B, Baricco M. Thermodynamic modelling of $Mg(BH_4)_2$. J Alloys Compd 2015;645:S64–8.
[115] Huot J, Liang G, Schulz R. Mechanically alloyed metal hydride systems. Appl Phys A Mater Sci Process 2001;72:187–95.
[116] Oelerich W, Klassen T, Bormann R. Metal oxides as catalysts for improved hydrogen sorption in nanocrystalline Mg-based materials. J Alloys Compd 2001;315:237–42.
[117] Barkhordarian G, Klassen T, Bormann R. Fast hydrogen sorption kinetics of nanocrystalline Mg using Nb_2O_5 as catalyst. Scr Mater 2003;49:213–7.
[118] Bogdanovic B, Schwickardi M. Ti-doped alkali metal aluminium hydrides as potential novel reversible hydrogen storage materials. J Alloys Compd 1997;253–254:1–9.
[119] Pitt MP, Vullum PE, Sorby MH, Emerich H, Paskevicius M, Webb CJ, et al. Hydrogen absorption kinetics and structural features of NaAlH4 enhanced with transition-metal and Ti-based nanoparticles. Int J Hydrogen Energy 2012;37:15175–86.
[120] Graetz J, Hauback BC. Recent developments in aluminum-based hydrides for hydrogen storage. MRS Bull 2013;38:473–9.
[121] Li H-W, Yan Y, Orimo S-i, Züttel A, Jensen CM. Recent progress in metal borohydrides for hydrogen storage. Energies 2011;4:185–214.
[122] Rönnebro E. Development of group II borohydrides as hydrogen storage materials. Curr Opin Solid State Mater Sci 2011;15:44–51.
[123] Humphries TD, Kalantzopoulos GN, Llamas-Jansa I, Olsen JE, Hauback BC. Reversible hydrogenation studies of NaBH4 milled with Ni-containing additives. J Phys Chem C 2013;117:6060–5.
[124] Minella CB, Pellicer E, Rossinyol E, Karimi F, Pistidda C, Garroni S, et al. Chemical state, distribution, and role of Ti- and Nb-based additives on the $Ca(BH_4)_2$ system. J Phys Chem C 2013;117:4394–403.
[125] Al-Kukhun A, Hwang HT, Varma A. NbF5 additive improves hydrogen release from magnesium borohydride. Int J Hydrogen Energy 2012;37:17671–7.
[126] Bardaji EG, Hanada N, Zabara O, Fichtner M. Effect of several metal chlorides on the thermal decomposition behaviour of alpha-$Mg(BH_4)_2$. Int J Hydrogen Energy 2011;36:12313–8.
[127] Chen J, Zhang Y, Xiong Z, Wu G, Chu H, He T, et al. Enhanced hydrogen desorption from the Co-catalyzed LiBH4–$Mg(BH_4)_2$ eutectic composite. Int J Hydrogen Energy 2012;37:12425–31.
[128] Zhang ZG, Wang H, Liu JW, Zhu M. Thermal decomposition behaviors of magnesium borohydride doped with metal fluoride additives. Thermochim Acta 2013;560:82–8.
[129] Saldan I, Campesi R, Zavorotynska O, Spoto G, Baricco M, Arendarska A, et al. Enhanced hydrogen uptake/release in 2LiH-MgB2 composite with titanium additives. Int J Hydrogen Energy 2012;37:1604–12.
[130] Matsumura D, Ohyama T, Okajima Y, Nishihata Y, Li H-W, Orimo S. Correlation between structure of titanium additives and dehydrogenation reaction of magnesium borohydride studied by continuous observation of X-Ray absorption spectroscopy. Mater Trans 2011;52:635–40.
[131] Wahab MA, Jia Y, Yang D, Zhao H, Yao X. Enhanced hydrogen desorption from $Mg(BH_4)_2$ by combining nanoconfinement and a Ni catalyst. J Mater Chem A 2013;1:3471–8.
[132] Ngene P, Verkuijlen MHW, Zheng Q, Kragten J, van Bentum PJM, Bitter JH, et al. The role of Ni in increasing the reversibility of the hydrogen release from nanoconfined LiBH4. Faraday Discuss 2011;151:47–58.
[133] Zhang Y, Liu Y, Pang Y, Gao M, Pan H. Role of Co3O4 in improving the hydrogen storage properties of a $LiBH_4$-$2LiNH_2$ composite. J Mater Chem A 2014;2:11155–61.
[134] de Jongh PE, Allendorf MD, Vajo JJ, Zlotea C. Nanoconfined light metal hydrides for reversible hydrogen storage. MRS Bull 2013;38:488–94.
[135] Au YS, Yan Y, de Jong KP, Remhof A, de Jongh PE. Pore confined synthesis of magnesium Boron hydride nanoparticles. J Phys Chem C 2014;118:20832–9.
[136] Sartori S, Knudsen KD, Zhao-Karger Z, Bardaji EG, Muller J, Fichtner M, et al. Nanoconfined magnesium borohydride for hydrogen storage applications investigated by SANS and SAXS. J Phys Chem C 2010;114:18785–9.
[137] Yan Y, Au YS, Rentsch D, Remhof A, de Jongh PE, Züttel A. Reversible hydrogen storage in $Mg(BH_4)_2$/carbon nanocomposites. J Mater Chem A 2013;1:11177–83.
[138] Capurso G, Agresti F, Crociani L, Rossetto G, Schiavo B, Maddalena A, et al. Nanoconfined mixed Li and Mg borohydrides as materials for solid state hydrogen storage. Int J Hydrogen Energy 2012;37:10768–73.
[139] Colognesi D, Ulivi L, Zoppi M, Ramirez-Cuesta AJ, Orecchini A, Karkamkar AJ, et al. Hydrogen-storage materials dispersed into nanoporous substrates studied

through incoherent inelastic neutron scattering. J Alloys Compd 2012;538:91–9.
[140] Ingleson MF, Barrio JP, Bacsa J, Steiner A, Darling GR, Jones JTA, et al. Magnesium borohydride confined in a metal-organic framework: a preorganized system for facile arene hydroboration. Angew Chem Int Ed 2009;48:2012–6.
[141] Javadian P, Jensen TR. Enhanced hydrogen reversibility of nanoconfined LiBH4-$Mg(BH_4)_2$. Int J Hydrogen Energy 2014;39:9871–6.
[142] Hino S, Fonnelop JE, Corno M, Zavorotynska O, Damin A, Richter B, et al. Halide substitution in magnesium borohydride. J Phys Chem C 2012;116:12482–8.
[143] Jepsen LH, Ban V, Moller KT, Lee Y-S, Cho YW, Besenbacher F, et al. Synthesis, crystal structure, thermal decomposition, and B-11 MAS NMR characterization of $Mg(BH_4)_2(NH_3BH_3)_2$. J Phys Chem C 2014;118:12141–53.
[144] Roedern E, Jensen TR. Thermal decomposition of $Mn(BH_4)_2$-$m(BH_4)_x$ and $Mn(BH_4)_2$-MH_x Composites with M = Li, Na, Mg, and Ca. J Phys Chem C 2014;118:23567–74.
[145] Jepsen LH, Ley MB, Lee Y-S, Cho YW, Dornheim M, Jensen JO, et al. Boron–nitrogen based hydrides and reactive composites for hydrogen storage. Mater Today 2014;17:129–35.
[146] Paskevicius M, Ley MB, Sheppard DA, Jensen TR, Buckley CE. Eutectic melting in metal borohydrides. PCCP 2013;15:19774–89.
[147] Kalantzopoulos GN, Vitillo JG, Albanese E, Pinatel E, Civalleri B, Deledda S, et al. Hydrogen storage of Mg–Zn mixed metal borohydrides. J Alloys Compd 2014;615(Suppl. 1):S702–5.
[148] Albanese E, Civalleri B, Casassa S, Baricco M. Investigation on the decomposition enthalpy of novel mixed $Mg_{(1-x)}Zn_x(BH_4)_2$ borohydrides by means of periodic DFT calculations. J Phys Chem C 2014;118:23468–75.
[149] Albanese E, Kalantzopoulos GN, Vitillo JG, Pinatel E, Civalleri B, Deledda S, et al. Theoretical and experimental study on $Mg(BH_4)_2$–$Zn(BH_4)_2$ mixed borohydrides. J Alloys Compd 2013;580(Suppl. 1):S282–6.
[150] Muldoon J, Bucur CB, Oliver AG, Sugimoto T, Matsui M, Kim HS, et al. Electrolyte roadblocks to a magnesium rechargeable battery. Energy Environ Sci 2012;5:5941–50.
[151] Xu C, Chen Y, Shi S, Li J, Kang F, Su D. Secondary batteries with multivalent ions for energy storage. Sci Rep 2015:5.
[152] Matsuo M, Nakamori Y, Orimo S-i, Maekawa H, Takamura H. Lithium superionic conduction in lithium borohydride accompanied by structural transition. Appl Phys Lett 2007:91.
[153] Maekawa H, Matsuo M, Takamura H, Ando M, Noda Y, Karahashi T, et al. Halide-stabilized $LiBH_4$, a room-temperature lithium fast-ion conductor. J Am Chem Soc 2009;131:894.
[154] Unemoto A, Matsuo M, Orimo S-i. Complex hydrides for electrochemical energy storage. Adv Funct Mater 2014;24:2267–79.
[155] Cerny R, Schouwink P, Sadikin Y, Stare K, Smrcok Lu, Richter B, et al. Trimetallic borohydride $Li_3MZn_5(BH_4)_{15}$ (M = Mg, Mn) containing two weakly interconnected frameworks. Inorg Chem 2013;52:9941–7.
[156] Matsuo M, Oguchi H, Sato T, Takamura H, Tsuchida E, Ikeshoji T, et al. Sodium and magnesium ionic conduction in complex hydrides. J Alloys Compd 2013;580:S98–101.
[157] Aurbach D, Lu Z, Schechter A, Gofer Y, Gizbar H, Turgeman R, et al. Prototype systems for rechargeable magnesium batteries. Nature 2000;407:724–7.
[158] Matsui M. Study on electrochemically deposited Mg metal. J Power Sources 2011;196:7048–55.
[159] Aurbach D, Cohen Y, Moshkovich M. The study of reversible magnesium deposition by in situ scanning tunneling microscopy. Electrochem Solid State Lett 2001;4:A113–6.
[160] Connor JH, Reid WE, Wood GB. Electrodeposition of metals from organic solutions. 5. Electrodeposition of magnesium and magnesium alloys. J Electrochem Soc 1957;104:38–41.
[161] Mohtadi R, Matsui M, Arthur TS, Hwang S-J. Magnesium borohydride: from hydrogen storage to magnesium battery. Angew Chem Int Ed 2012;51:9780–3.
[162] Tuerxun F, Abulizi Y, NuLi Y, Su S, Yang J, Wang J. High concentration magnesium borohydride/tetraglyme electrolyte for rechargeable magnesium batteries. J Power Sources 2015;276:255–61.
[163] Su S, Huang Z, Nuli Y, Tuerxun F, Yang J, Wang J. A novel rechargeable battery with a magnesium anode, a titanium dioxide cathode, and a magnesium borohydride/tetraglyme electrolyte. Chem Commun 2015;51:2641–4.
[164] Chang J, Haasch RT, Kim J, Spila T, Braun PV, Gewirth AA, et al. Synergetic role of Li+ during Mg electrodeposition/dissolution in borohydride diglyme electrolyte solution: voltammetric stripping behaviors on a Pt microelectrode indicative of Mg-Li alloying and facilitated dissolution. ACS Appl Mater Interfaces 2015;7:2494–502.
[165] Farina L, Munao D, Silvestri L, Panero S, Meggiolaro D, Brutti S, et al. Environment and electrical engineering. In: IEEE 15th International Conference 2015; 2015. p. 1827–32.
[166] Mohtadi R, Mizuno F. Magnesium batteries: current state of the art, issues and future perspectives. Beilstein J. Nanotechnol 2014;5:1291–311.